Design of the Battery Restraining System and the Motor Mounting system for the REV Jet Ski

Rajinda Jayamanna

20240104
School of Mechanical and Chemical Engineering
University of Western Australia

Supervisor: Prof. Thomas Braunl

School of electrical and Electronic Computer Engineering
University Of Western Australia

ABSTRACT

In Australia there is an increasing awareness for global warming, and its effects on the environment. Therefore there is a great need to develop renewable energy technology and demonstrate its viability to the general public. Australia's heavy dependence on gasoline base transportation produces large amounts of greenhouse gases, thus an alternative must be provided through research and promotion of electric drive technology.

This project is responsible for the design, construction and placement of the battery restraining system and the motor mounting system for the REV Jet Ski. Design and placement is dependent upon many factors such as weight distribution, available space and cost constraints. The design of the battery restraining system and the motor mounting system will follow any relevant standard and regulation. The design of these components will be aided by Solid Works design package and ANSYS Workbench. Upon successfully completing the design and stress analysis the battery restraining system and the motor mounting system will be fabricated and assembled through the mechanical engineering workshop or the physics work shop.

This project also evaluated g forces that a Jet Ski experience at peak performance. This was achieved through attaching a USB accelerometer in the hull of the REV Jet Ski. The data obtained from the experiment provided crucial information in moving forward with the battery restraining system and the motor mounting.

Acknowledgements

I would like to extend my thanks to the following personnel for their continued support and interest in this project.

Professor Thomas Braunl for his support and advice on the design of the battery restraining system.

Brett Manners of TMT for providing assistance and insight on the design issues.

Dick Haffenden from Submersible Motors Engineering for assisting the REV Jet Ski team with the design of the motor mounting system.

Thanks also to the REV Jet Ski team members for their continued support

And finally thanks goes to my family and friend for their support and understanding.

Contents

ABSTRACT 1

Letter of Transmittal 2

Acknowledgements 3

Table of Figures 7

List of Tables 9

Nomenclature 10

1. Introduction 11

1.1 Background 11

1.2 Project Objective 12

2 Literature Survey 12

2.1 Chapter Overview 12

2.2 Electric Drive Technology in the Automotive Industry 12

2.1.2 Electric Drives Watercraft 14

2.1.3 Motor 15

2.1.4 Battery Cage Impact Requirements 15

2.1.5 Battery restraining system 16

3. Surface Modelling of the REV Jet Ski 17

3.1 Overview 17

3.2 Methodology 18

3.2.1 Initial method 18

3.2.2 Final method 19

3.3 Front and aft section surface map 20

4. Determination of Impact forces 21

4.1 Overview 21

4.2 Methodology 22

4.3 Operating the accelerometer 24

4.3.1 Relevant Features 24

4.3.2 Configuration of X16-1C accelerometer 26

4.3.3 Operating Instructions 28

4.4 Results and Discussion 29

4.4.1 Results 29

4.4.2 Discussion 33

5. Battery Restraint System Design for the Jet Ski 34
5.1 Overview 34
5.2 Design Process 34
5.2.1 Battery Restraining System Design Requirements 34
5.2.2 Constraints 35
5.2.3 Battery Specification 36
5.2.4 Design Software 39
5.2.5 Design Methodology 39
5.2.5 Safety 41
5.3 Results and Discussion 42
5.3.1 Battery restraining system location and battery arrangement 42
5.3.2 Material Selection 45
5.3.3 Battery box design 46
5.3.4 Stress Analysis. 51
5.3.5 Finite element analysis of the battery box 53
5.3.6 Summary 62
5.3.7 Limitation of Finite element Analysis 62
5.3.8 Fabrication 62
6 Design of the motor mounting system 63
6.1 Overview 63
6.2 Design Methodology 63
6.2.1 Design requirement for the motor mounting system 63
6.2.2 Design process 63
6.3 Initial design and final design 64
6.3.1 Initial design 64
6.3.2 Final design and discussion 66
7 Conclusion and future works 68
8 References 69
Appendix A Card Board Profiles 71
Appendix B 73
Appendix C 74
Appendix D 75
Appendix E 77

Table of Figures

Figure 1 AC induction motor system ... 13
Figure 2 DC motor system ... 14
Figure 3 REV Jet Ski ... 17
Figure 4 Front section of the Jet Ski ... 17
Figure 5 Aft section of the Jet Ski ... 18
Figure 6 Card board profile allignment ... 19
Figure 7 Surface model of the aft section ... 20
Figure 8 Surface model of the front section ... 21
Figure 9 Mounting point for the accelerometer ... 23
Figure 10 GCDC X16-1C ... 24
Figure 11 G-force (g) vs. Time (s) ... 25
Figure 12 Config.text file for 50Hz ... 27
Figure 13 Config.text file for 100Hz ... 27
Figure 14 Accelerometer assembly ... 28
Figure 15 Coordinate system for the accelerometer ... 30
Figure 16 G-force recorded in the z axis ... 31
Figure 17 G-force recorded in the x axis ... 32
Figure 18 G-force recorded in the y axis ... 33
Figure 19 ThunderSky TS-LFP100AHA ... 36
Figure 20 Headway 10Ah ... 37
Figure 21 Battery Module ... 38
Figure 22 Dimensions for the battery module ... 38
Figure 23 Design flow chart ... 40
Figure 24 Initial battery module arrangement ... 43
Figure 25 Revised configuration for layer 1 ... 44
Figure 26 Revised configuration for layer 2 and layer 3 ... 45
Figure 27 initial design proposal ... 47
Figure 28 Exploded view of the initial design ... 47
Figure 29 Final Design ... 49
Figure 30 Exploded view of the final design ... 49
Figure 31 Aluminum I-beam profile (One Steel 2013) ... 50
Figure 32 Total deformation, front impact, layer 1 ... 53
Figure 33 safety factor, front impact, layer 1 ... 54
Figure 34 Total deformation side Impact Layer 1 ... 55
Figure 35 Safety factor, side impact, layer 1 ... 55
Figure 36 Total deformation, vertical impact, layer 1 ... 56
Figure 37 Safety factor, vertical impact, layer1 ... 57
Figure 38 Total deformation, front impact, layer 2 ... 58
Figure 39 safety factor, front impact, layer 2 ... 58
Figure 40 Total deformation, side impact, layer 2 ... 59
Figure 41 Safety factor, side impact, layer 2 ... 60
Figure 42 Total deformation, vertical impact, and layer 2 ... 61
Figure 43 Safety factor, vertical impact, and layer 2 ... 61
Figure 44 Initial design for the motor mounting system ... 65
Figure 45 Aft view ... 66
Figure 46 Final design ... 67

Figure 47 Profile 1 Origin 71
Figure 48 Profile 2 71
Figure 49 Profile 3 72
Figure 50 Dimensions for the surface map. 73
Figure 51 Support Frame design 74
Figure 52 Support mount Vertical Impact of 10g 74
Figure 53 Motor mounting system and the motor 75
Figure 54 Bracket Design for mounting point 3 76
Figure 55 Data sheet for adhesive tapes 77

List of Tables

Table 1 NCOP Impact requirement for battery restraining system 15
Table 2 Impact requirement for the battery restraining system and the motor mounting system 34
Table 3 Headway 10Ah batteries 37
Table 4 Material properties from Standards Australia 1997 46
Table 5 Required Pressure 52

Nomenclature

$A_{channel}$	Surface area of the channel beam (m^2)
a	Acceleration
AC	Alternating current
CNC	Computer Numerical Control
DC	Direct Current
F	Force (N)
FEA	Finite Element Analysis
I	Current (A)
ICE	Internal Combustion Engine
m	Mass (kg)
P	Pressure (Pa)
PC	Personal Computer
PWC	Personal Water Craft
REV	Renewable Energy Vehicle
ROV	Remotely Operated Vehicle
SME	Submersible Motors Engineering
TMT	Total Marine Engineering

1. Introduction

1.1 Background

In Australia and around the world, the internal combustion engine has been the norm for powering personal watercrafts such as the Jet Ski. With increased restrictions for carbon emissions, and noise pollution, the ICE (internal Combustions Engine) Jet skis are becoming unviable to be used as a personal watercraft for recreational purposes. Many environmental studies conducted in Australia have concluded that fossil fuel based transports causes significant disturbance to the local environment (Pachauri, RK & Reisinger, A 2007). The ICE Jet ski has also been shown to contribute to water and air pollution. In order to demonstrate a solution to the current pollution issues caused by the ICE Jet ski, the UWA REV team has planned to convert ICE Jet Ski into an emission free electric Jet Ski.

At the current stage, there are very few case studies for electric conversion of ICE Jet Skis. To compensate for the lack of specific case studies, electric conversion techniques for road vehicles will be adopted and modified to be viable and safe for a watercraft. Electric conversions of road vehicles are a fairly popular phenomenon in many European countries (Tan, D. 2008). Although it is still very rare in Australia, the concept is increasingly becoming popular due to increased fossil fuel prices and increased public awareness of the effects of greenhouse gases on the environment (Hooper, I. 2011). An electric vehicle is mainly powered by battery cells. Although battery electric vehicle are more efficient and do not pollute the environment, there are many performance challenges. Electric vehicles typically have a range of 200km or below, which is much lower than its ICE counterparts. The Electric vehicle would also have a charge time of 3 to 10 hours depending on the type of the charging station (Brant, B 1994), The costs of the batteries are typically expensive and must be replaced every 5-8 years. These common limitations for the electric vehicle can be applied to an electric watercraft as well.

The REV Jet Ski team consisting of 6 students from the school of electrical engineering and mechanical engineering aims to tackle the challenges of building an electric personal watercraft which produces no pollution and perform as well as the petrol engine counterparts. This project hopes to demonstrate to the community that electric drive technology is becoming a viable source of transport technology.

1.2 Project Objective

The aim of this project is to design and fabricate a functional battery restraining system and a motor mounting system. In order accomplish this goal the following objectives must be accomplished.

- Conduct research on existing battery restraining technology and motor mounting systems.
- Develop a 3D model of the inside surface of the hull.
- Measure the g-force experienced by a petrol engine Jet Ski and compares the results to current standards and regulation on impact requirements for electric vehicles. Come to a conclusion on the appropriateness of applying automotive standards to watercrafts.
- Create prototype models for the battery restraining system and the motor mounting system.
- Investigate the reliability of the designs using finite element stress analysis.

2 Literature Survey

2.1 Chapter Overview

This chapter explores the existing concepts and designs for electric drive boats, yachts and road going vehicles. Current designs and concepts for battery restraining systems in cars and boats will also be discussed.

2.2 Electric Drive Technology in the Automotive Industry

Increasing public interest in environmental issues has made the electric drive technology to become increasingly popular in Australia. It is predicted the sales of electric vehicles will improve as the infrastructure to support electric vehicles are established. Electric drive technology has several advantages over conventional drive trains. An electric drive train emits far less pollutants than its fossil fuel powered counterparts and electric cars can be far more convenient as it can be charged from a standard power outlet of a home.

The major disadvantage of electric vehicles is its range. For example the Holden Volt, a small electric car sold in Australia has a range of approximately 70km. This range is far less than a conventional vehicle in its class which may have a range of 320km to 480km (Brant, B 1994), Electric drive technology in automobiles is commonly categorized into two key areas. They are the automobiles using AC induction motor as their power train and those that uses DC electric motors.

A schematic for a typical AC induction motor system in an electric vehicle is shown fig ().

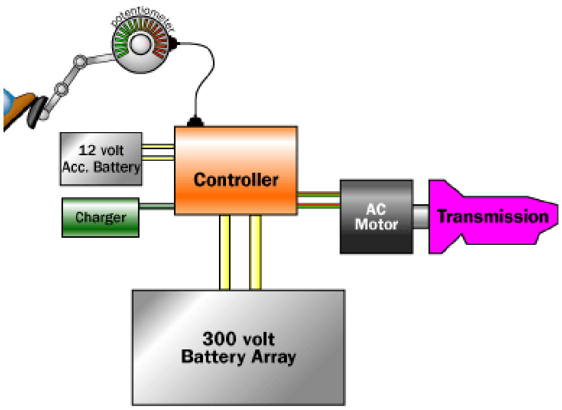

Figure 1 AC induction motor system

The AC induction motor is given and alternating current, created through the motor controller shown in fig (). The controller draws DC current from the battery array and creates three pseudo-sine waves by pulsing on and off. AC induction motor system requires a few critical components listed below.

- Charger
- External power source to power the AC controller
- DC-DC converter used to recharge the external power source
- Batteries
- Battery restraining system.

A schematic of a typical DC motor system used for road going vehicles are shown below.

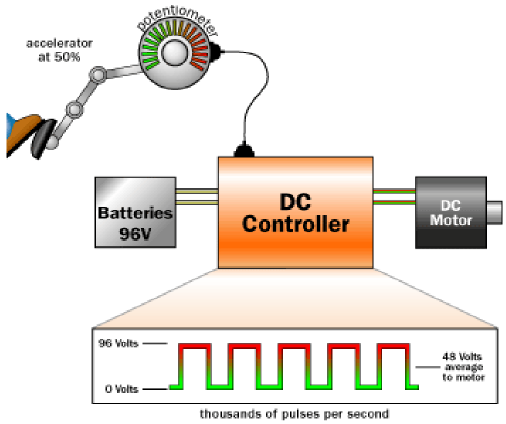

Figure 2 DC motor system

In the DC motor system, the DC controller draws power from the batteries and delivers the power directly to the motor. However the controller is also connected to potentiometers (variable resistors). The potentiometers determine how much power is required to be delivered to the motor. The controller is able to deliver zero power or full power and any power level in-between.

2.1.2 Electric Drives Watercraft

Electric drive boats are increasingly becoming popular due to its vast advantages over conventional drive watercrafts (Mathys, C 2004). Whilst the conventional watercrafts are cheaper and have a larger operational range, the electric drive watercrafts are easy to maintain, highly reliable and free of vibration problems. Electric drive watercrafts are also emission free, thus it is an environmentally friendly alternative to a conventional watercrafts.

Currently in Australia, there are several boating construction companies involved in the manufacture of electric boats. Eco Boat Australia is one such company offering small to medium sized leisure boats starting from AUD$25,000.

According to electric parts and motors suppliers as EV Works and ALTRONICS, personal conversions of conventional watercraft into electric drive watercrafts are also becoming a popular trend.

As of 2013 there has been no attempt to create a fully functioning electric drive jets ski which matches the performance figures of a conventional jet ski.

2.1.3 Motor

In choosing an appropriate motor system for the Jet Ski, the AC induction motor and DC motors were considered. The potential motor must be able to output 50kW, at 96V and it must also be able to reach a shaft speed of 7500RPM. The power rating of 50kW was decided upon due to its comparable rating with the original motor. A voltage rating of 96V was adopted as part of the requirement for the electric motor. This was due to the advice of the supervisors that any electrical components with a voltage rating of 115V and above required a professional electrician to install and operate. The previous petrol motor also had a maximum shaft speed of 7000RPM to 8000RPM, thus this motor shaft speed was also adopted as a requirement for the electric motor.

2.1.4 Battery Cage Impact Requirements

In the automotive industry, there are various standards outlining the impact requirements for a battery restraining system. The REV Hyundai Getz and REV Lotus Elise had to be complied with the appropriate standards to be registered as road worthy vehicles. The REV vehicles were classified as individually constructed passenger vehicles, and had to be complied with Australian Design Rules and Individually Constructed Vehicles.

The specific impact requirements for the battery restraining system were designated in the National Guidelines for the Installation of Electric Drive in Motor Vehicles (NCOP14). This standard is found within the National Code of Practice for Light Vehicle Construction (NCOP).

NCOP14 states that the batteries used in the vehicles must be fixed in position so that all degrees of freedom are constrained. The batteries must be housed within a battery restraining system that is capable of withstanding vehicle crash acceleration shown in table 1.

Table 1 NCOP Impact requirement for battery restraining system

Impact Surface	Impact Requirement
Front Impact	20g
Side Impact	15g
Vertical Impact	10g
Rear Impact	10g

In other words, a battery restraining system designed though the NCOP14 standards must be able to withstand a front impact force of 20 times the gravity of the mass of the batteries.

The NCOP14 standard also stipulates that batteries containing liquid or produces gas must be sealed from the passenger compartment of the vehicle so that neither liquid nor gas will leak into the interior of the vehicle. According to the type of batteries, NCOP14 recommend to seal the battery compartment, individually seal the batteries or design a ventilation system that can vent the gases produced directly to the atmosphere.

Upon further inspection of the regulations, it was found that the regulations for the sealed battery restraining system is only applicable for lead acid batteries as they can produce hydrogen and oxygen gas during charging.

The regulations further outlines that the batter restraining system must be fabricated through corrosion resistant materials or the system must be coated by materials that are resistant to cracking or shrinking under vibrations and temperature fluctuations.

Other miscellaneous standards and regulations that a vehicle must comply with or consider include labeling of the battery compartment with appropriate hazard symbols. The symbols must also indicate the likely voltage that may be encountered from the component.

2.1.5 Battery restraining system

A battery restraining system is used to restrain the batteries in place during normal operation of an electric vehicle as well as during a collision or a rollover. (Brown 1993) states that the minimum dimensions for the battery restraining system should be no less than 4.8mm thick and 38.1mm wide. If the battery restraining system is especially large, reinforcing straps are required to support the batteries. Angle stocks are most commonly used for battery restraining system along with bars and rigid straps. If the bars and rigid straps are made of metal, they must be placed carefully to prevent short circuit along two terminals (Brown 1993)

3. Surface Modelling of the REV Jet Ski

3.1 Overview

Figure 3 REV Jet Ski

The REV Jet Ski shown in fig 3 must house large number of mechanical and electrical equipment within its hull. Major components such as the motor, motor mounting system, battery restraining system, controller, and battery management system require placement within the hull in a manner which is safe and maximize the performance of the Jet Ski. The REV Jet ski contains 3 major mounting points in the aft section and 2 minor mounting points in the front section. The minor mounting points are shown in fig 4 and the 3 major mounting points are shown in fig 5.

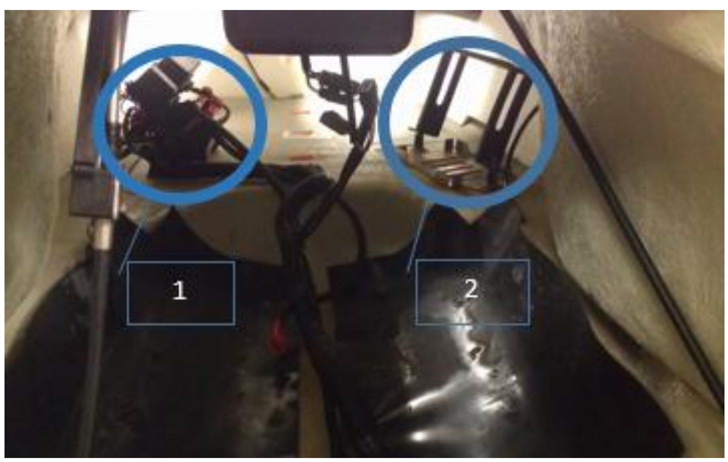

Figure 4 Front section of the Jet Ski

As it can be seen from fig 4, the minor mounting points have been located far to the front of the Jet Ski. Mounting point 1 is located on the front left hand side of the Jet Ski and currently used to restrain the fuse box. To use this mounting point, the fuse box must be removed and a rubber mount must be installed. Mounting point 2 is located on the front right hand side, it was used previously to restrain a 12V lead acid battery which supplied power to the electrical systems in the Jet Ski. To use mounting point 2, the frame shown in fig 4 must be removed and replaced with rubber mounting points.

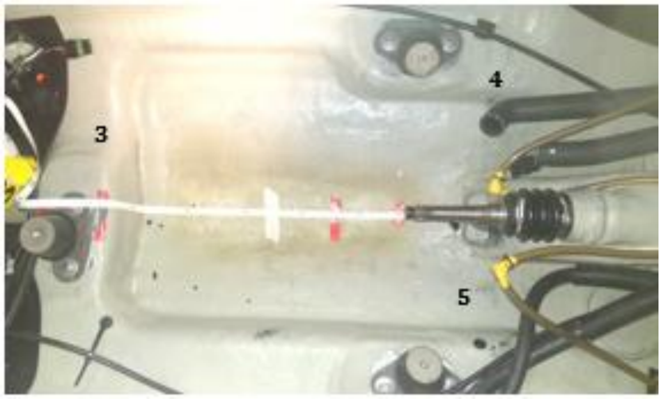

Figure 5 Aft section of the Jet Ski

Fig 5 shows the 3 major mounting points in the aft section of the Jet Ski. Mounting points 3, 4 and 5 have been previously used to support the petrol motor. Mounting point 3 was also used to support a part of the Jet Ski's fuel tank.

In order to place the mechanical and electrical equipment, the exact locations of the mounting points and the contours inside the hull must be mapped accurately. The information gathered can be used to develop 3D model of the inside of the hull. The model can be used for various purposes by the REV Jet Ski team, however for this project, it can be used to determine the placement for the battery restraining system and the motor mounting system. In the following section, the methods considered to develop the model will be discussed.

3.2 Methodology

3.2.1 Initial method

In developing a 3D model of the inside of the hull of the Jet Ski, 2 methods were considered. The first method proposed was to use laser scanners to scan the outside contours of the hull and subsequently scanning the inside of the hull of the Jet Ski. The laser scanners can then develop 3D image of the Jet Ski with a high degree of accuracy. The 3D image produced is also compatible with various engineering software such as Solid Works design package and the ANSYS workbench. This method would be ideal in developing a 3D model of the inside surface of the Jet Ski, however the task of developing a model of the inside of the Jet Ski was placed a low priority in comparison to the design and construction of the battery restraining system and the motor mounting system. Thus the REV program did not support the 3D scanner method as the resources could be spent elsewhere on critical tasks

3.2.2 Final method

The second and final method considered for the development of the 3D model was to manually measure key dimensions of the Jet Ski and develop cardboard profiles to match the contours of the hull. The card board profiles that were developed for the aft section of the REV Jet Ski are shown in Appendix A. The profile seen in Appendix A, fig 47 was developed to match the contours between 0cm to 20cm, measured from mounting point 3 (mounting point shown in fig 5). The second profile developed was created to match the contours between 20cm to 32cm in the aft section (shown in appendix A, fig 48). And finally, the 3rd profile was developed for the contours between 32cm to 56cm in the aft section of the REV Jet Ski. The cardboards profiles developed are aligned in the Jet Ski as shown in fig 6.

Figure 6 Card board profile allignment

Once the cardboard profile was developed to match the surface contours of the Jet Ski, Pictures of each of the profile was taken. The pictures were subsequently imported to the Solid Works design software using the import picture tool. Profile 1, 2, and 3 were placed at 0cm, 20cm and 32cm with respect to the origin as measured. The contour profile was then traced using the spline feature in the sketch tool bar. The sketch containing the traced contours was used to create an extruded part for each of the profile. The parts for each profile were later mated in the assembly feature.

The positions of the mounting points 4 and 5 were manually measured with respect to mounting point 3 (shown in fig 4). A rough 3D model of the mounting points was also included in the final surface map.

A similar procedure was followed in developing a surface contour map for the front section of the Jet Ski. The final surface map of the front section and the aft section is shown in the next section.

3.3 Front and aft section surface map

The methodology described in section 3.2.2 was used to create 3D model of the inside surface of the Jet Ski. The aft section and the front section surface maps are shown in fig 7 and fig 8. The surface map of the front and aft section can be used to conceptualize the placement of electrical and mechanical equipment placement. The surface models can also be used as a guide on the positions of the mounting point. The dimensions for the surface models are shown in Appendix B, fig 50. During the development of the surface model, it was found that the mounting points located in the aft section are not symmetric. Mounting point 3 was measured to be approximately 15mm away from the centerline of the Jet Ski.

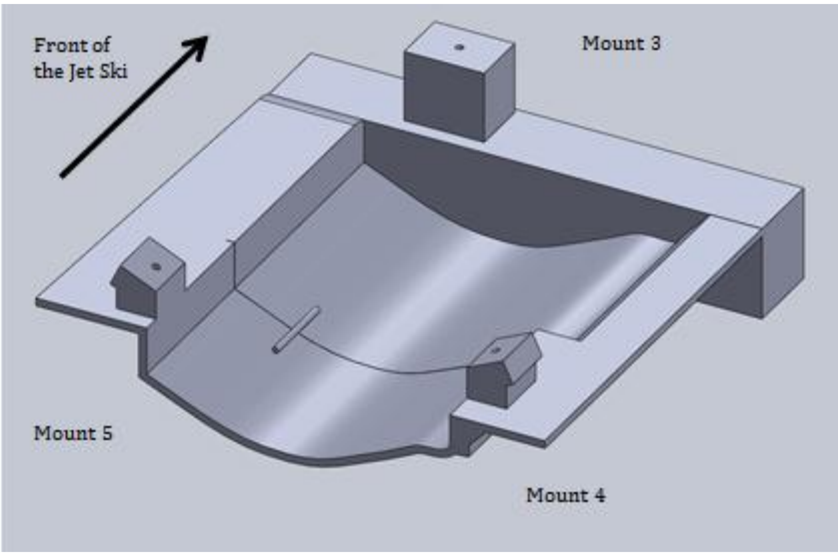

Figure 7 Surface model of the aft section

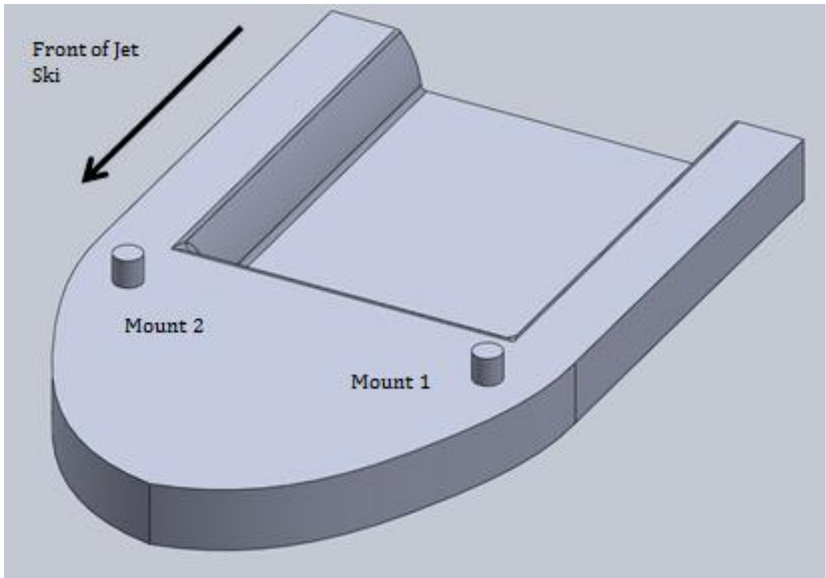

Figure 8 Surface model of the front section

It was also found that mounting point 4 and 5 were not aligned. This information became crucial in designing the motor mounting system and the battery restraining system as it has prevented misalignment of brackets and mounting structures.

Although the surface maps have been created using cardboard profiles, the models are estimated to have an error of 10 to 20 mm. This is due to inconsistencies arising from measuring error. To prevent the inconsistencies, the REV Jet Ski team members have taken turns on measuring critical distances such as distance between mount 1 and mount 2 as well as mount 5 and mount 4. Ultimately this procedure minimized measuring error and the models were refined to fit the new measurements.

4. Determination of Impact forces

4.1 Overview

The electric drive Jet Ski designed by the REV program is one of the first attempts made into converting a conventional Jet Ski into electric drive. Thus relevant standard and regulation used for this activity was difficult to obtain. In designing the battery restraining system and the motor mounting system, the most relevant standards for impact was found in NCOP14 (national code of practice for light vehicle construction). This standard stipulates the battery restraining system must withstand a front impact force of 20g, side impact force of 15g, rear impact force of 10g and a vertical impact force of 10g.

The impact forces outlined in NCOP14 for the design of a battery restraining system is valid for a 1 time impact of a specified force, for example the battery restraining system must be able to withstand a front impact of 20g which is applied only once. This standard is most appropriate for an electric motor vehicle, where the force outlined in table 1 represent realistic impact scenario.

Through the extensive discussions with the REV Jet Ski and the marine safety officer, it was concluded that for an electric jet ski, it is inappropriate to design for the impact forces outlined in NCOP14 as it does not represent realistic impact forces experienced by a fast moving watercraft. It was also concluded that the forces experienced by a fast watercraft would be significantly lower than the impact forces outlined in NCOP14. Thus designing the battery restraining system through NCOP14 would result in the conclusion that using heavy, high strength material is more appropriate for housing the batteries.

For the purpose of designing the battery restraining system and the motor mounting system, it was necessary to determine realistic impact forces experienced by a watercraft. In order to determine impact forces, an experiment was devised to measure g forces experienced on an active conventional jet ski.

In the following section the detailed description of the experiment and the results obtained will be discussed. The design of the battery restraining system and the motor mounting system will be guided by the g force figures obtained through the experiment.

4.2 Methodology

In order to measure the impact forces experienced by an active Jet Ski, it was proposed to attach a portable USB accelerometer in the central glove compartment of the Jet Ski and operate the Jet Ski for a period time. The accelerometer will then record data of any g force experienced on the Jet Ski during operation. The proposed mounting point would be located just above the fuel tank and the central mounting point of the Jet Ski (see fig 4). This was considered to be an ideal location as the central mounting point will support the weight of the battery restraining system and the motor mounting system.

The experiment was conducted by hiring a SEADOO Jet Ski which is of the same class and weight of the REV Jet Ski. The conventional SEADOO Jet Ski was hired from Stag Watersports located in Mandurah and the experiment was carried out by one of the REV Jet Ski team members.

In order to perform the experiment effectively, the following procedures were devised and followed.

1. Input appropriate operating parameters into the accelerometer and follow the operating instructions outlined in section 3.3.3.
2. Complete safety induction for the SEADOO Jet ski (conducted through Stag Watersports)
3. Mount the accelerometer firmly to the central glove box compartment.
4. Operate the Jet Ski for 15 minutes.
5. Repeat step 1 with separate operating parameters. Then operate the Jet Ski for another 15 minutes.
6. Compile the data obtained from the accelerometer and plot the result to find the maximum g force experienced by the Jet Ski in all directions.

The above procedure was followed successfully to obtain reliable data of the impact g force experienced by the SEADOO Jet Ski. The results are discussed in section 3.4 and the data obtained can be found in Appendix C.

Figure 9 Mounting point for the accelerometer

4.3 Operating the accelerometer

The USB accelerometer used for the experiment was purchased online from Gulf Coast Data Concepts located in the United States. The specific model of accelerometer purchased for this experiment is Model X16-1C (see fig 10). This model is recommended by the manufacturer for applications such as vibration monitoring, monitoring the performance of automotive components and the monitoring of human motor activity (Gulf Coast Data Concepts 2007). This model was also found to be the least costly and the easiest to maintain. Thus it was concluded that using the X16-1C was the most appropriate and most cost effective method of capturing impact g force data.

Figure 10 GCDC X16-1C

4.3.1 Relevant Features

The relevant feature list for the X16-1C is shown below.

- Data logging in X, Y and Z axis
- Able to record g forces in the range of +/-16g
- Sample rate is user selectable, 12, 25, 50,100 and 200HZ sample rates are available.
- User designated dead band settings.
- Accurate time stamped data using Real Time Clock (RTC)
- Data recorded on to a removable SD card housed within the accelerometer (see fig)
- Data generated automatically onto excel spread sheets.
- Easily readable text files for operating parameters.
- Powered by a standard replaceable “AA” battery.

- Convenient on/off button

The features of X16-1C described above are ideal to undertake shock analysis of a Jet Ski in operation. The data logging feature of g forces experienced by the Jet Ski in all 3 axis is essential, as this information can be used to conduct a stress analysis on the battery restraining system and the motor mounting system. This accelerometer can also record large amount of G-forces (+/-16g). This was found to be an essential feature as there were no previous studies conducted on g forces experienced by watercrafts.

The X16-1C also allows the user to enter dead band settings where the user is able specify the minimum difference between recorded sensor readings. In other words, a new sample from the accelerometer sensor must exceed the previous recorded reading by a user specified value before the accelerometer outputs the data. This feature is further elaborated in fig 11.

Figure 11 G-force (g) vs. Time (s)

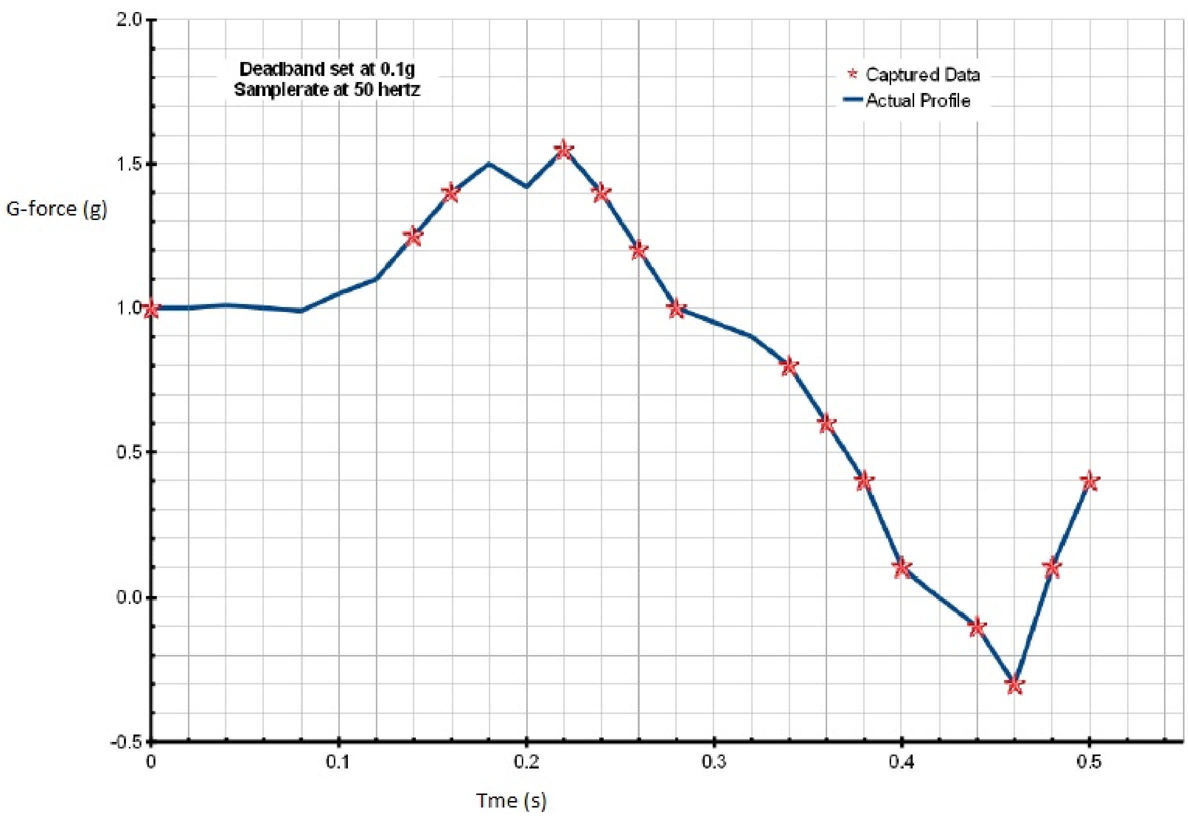

Fig 11 demonstrates the effect of the dead band setting. In fig 11 it can be seen that the dead band is specified by the user as 0.1g and the data sampling rate specified to be 50Hz. The red stars represents the captured data. It can be seen from figure 11 that regardless of the sampling rate, the difference between one captured points to another point is greater than 0.1g.

The dead band feature was used during the experiment to eliminate noise in the captured data sample. This feature will ensure the data obtained would be meaningful as there would be noticeable differences between the captured points.

4.3.2 Configuration of X16-1C accelerometer

As mentioned in section 4.3.1, the X16-1C can be configuring to have a sample rate or 12, 25, 50,100 or 200Hz. The accelerometer can also have a user defined dead bad setting to eliminate unwanted noise data (see section 4.3.1 for more details). For the purpose of collecting the impact data of the Jet Ski, a sample rate of 50Hz and 100Hz was used. A sample rate of 12 and 25Hz would significantly reduce the total data points recorded, thus it has the advantage of eliminating unwanted noise. However using a low sampling rate would also increase the probability of missing critical impact data points while recording. Using a higher sampling rate (e.g. 200Hz) would significantly increase the amount of data recorded. It would also increase unwanted noise. For this reason, in this particular experiment a sampling rate of 50Hz and 100Hz was used alongside a dead band setting of 0.005g. The dead band setting of 0.005g was chosen to eliminate data points with differences smaller than 0.005g (see section 4.3.1 for more information on dead band settings). This was deemed necessary as it was unlikely that the accelerometer would be able to accurately measure any impact forces to a degree of accuracy smaller than 0.005g. This setting would also assist in reducing the size of the collected data to a manageable size.

The configuration settings mentioned above can be programmed by plugging the USB accelerometer in to a PC and editing the config.text file located in the main directory of the micro-SD card. The relevant modification to the file is shown in fig 12.

```
; Jet ski impact data experiment
; Record constantly at 50Hz
samplerate = 50
; Record Motion > 0.005g
deadband = 5
; File Length
samplerateperfile = 50000
```

Figure 12 Config.text file for 50Hz

The configuration shown in fig 12 was used for the first 15 minutes of recording. As can be seen for the figure, the sample rate was set to 50Hz and the dead band setting is set to 0.005g. A limit to the file length was also created to manage the data sets.

```
; Jet ski impact data experiment
; Record constantly at 100Hz
samplerate = 100
; Record Motion > 0.005g
deadband = 5
; File Length
samplerateperfile = 50000
```

Figure 13 Config.text file for 100Hz

Similarly the configuration shown in fig 13 was used for the second 15 minutes. The accelerometer was configured for 100Hz with a dead band setting of 0.005g. The file length was also set at 50000. The results obtained for the experiment are shown and discussed in section 4.4.

4.3.3 Operating Instructions

The operating instruction for the X16-1C accelerometer is outlined below. The outlined steps were followed prior to conducting the experiment.

1. Disassemble the enclosure by unscrewing the 6inch Machine screw. Place an AA type battery into the battery holder with the positive battery terminal facing away from the USB connector. Reassemble the enclosure (Gulf Coast Data Concepts 2007). The assembly of X16-1C is shown in fig 14.

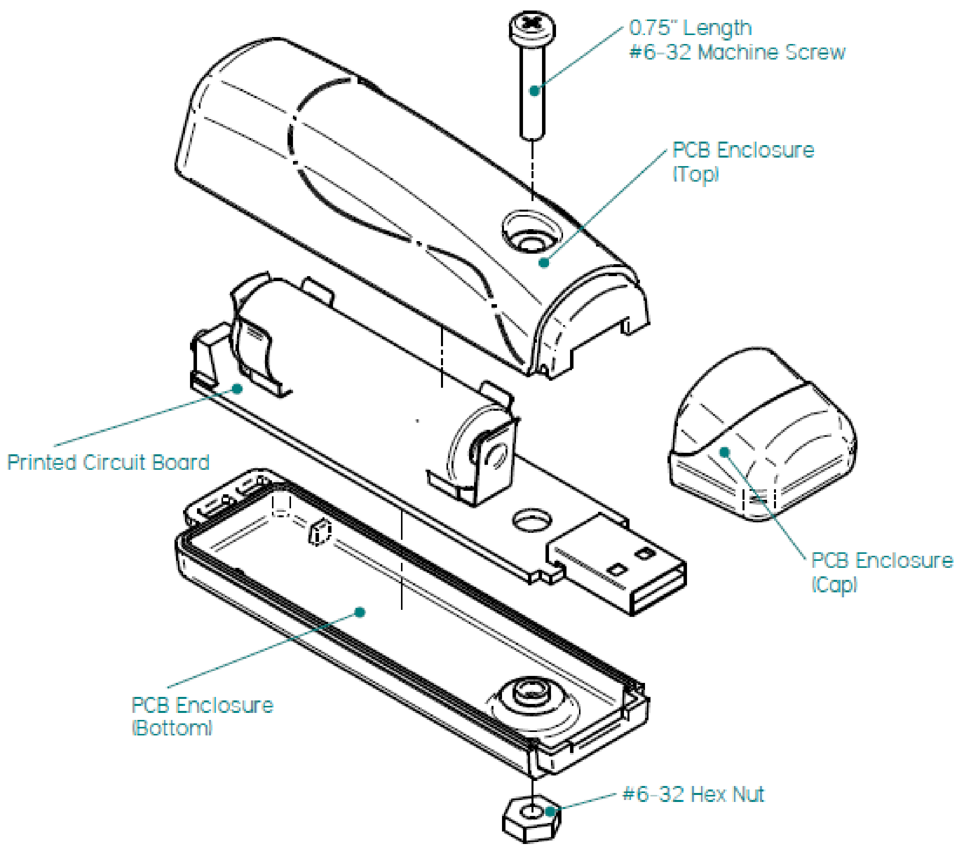

Figure 14 Accelerometer assembly

2. Insert the accelerometer into a PC and allow the OS to register the accelerometer as a mass storage device.
3. Configure the X16-1C accelerometer as seen from section 3.3.2. The configuration can be edited by changing the parameters on the config.text file located on the main directory of the accelerometer.

4. Unplug the X16-1C accelerometer from the PC and attach the device firmly on the target object. To attach the device, tape, or tie wraps can be used to mount the accelerometer.
5. Press the on Button located on the back of the accelerometer. The red LED will blink as the configuration file is accessed. Subsequently, the blue LED will blink at 1 second intervals indicating that the system is active and recording.
6. After recording, the system can be turned off by pressing the on button again.

Operating instructions were followed closely and the accelerometer was configured to the appropriate setting. The device was then mounted on the central glove compartment as mentioned in section 4.2. The accelerometer recorded the impact data in 2, 15 minute periods using 50Hz and 100Hz sample rates. Approximately 40000 reliable data points were collected from conducting the experiment. The results will be discussed in section 4.4

4.4 Results and Discussion

4.4.1 Results

The experiment yielded approximately 40000 impact data points using the 50Hz sampling setting. The data obtained was transferred to an excel spreadsheet and the results were plotted. As mentioned in section 4.2, the accelerometer is able to collect impact data in X, Y and Z direction. Thus a plot was developed for each direction showing the impact forces (g) plotted against time (s). The coordinate system employed by the accelerometer is shown in fig 15

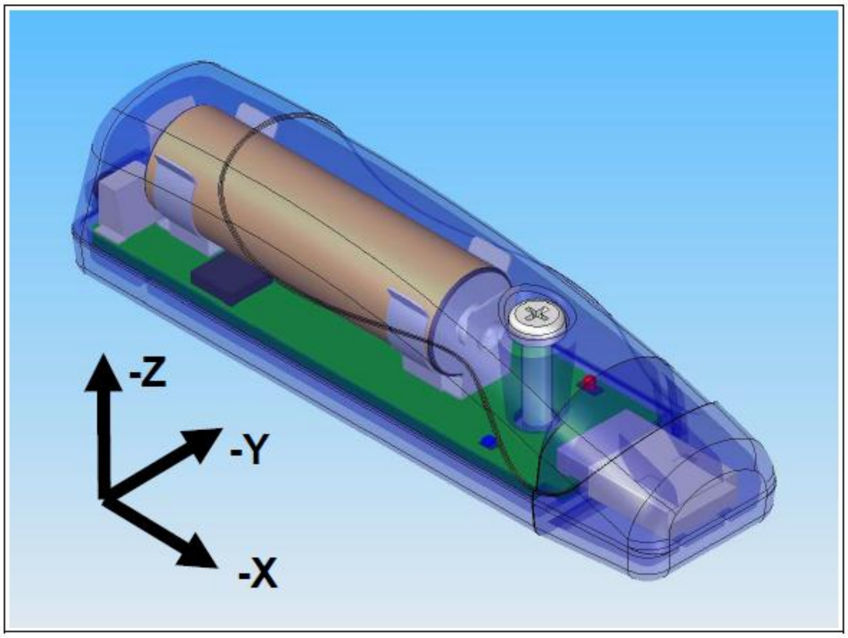

Figure 15 Coordinate system for the accelerometer

From fig 15 it can be seen that vertical impact experienced by the Jet Ski will be registered in the z axis. An impact in from the top of the Jet Ski will be registered as positive g force and an impact from the bottom of the Jet Ski will be registered as negative g force. Similarly, impact experienced from the left side of the Jet Ski will be registered as positive g force and impact from the right side will be registered as negative g force. Finally impact experienced from the front of the Jet Ski will be registered as negative g force and impact triggered from the rear of the Jet Ski will be recorded as positive g force.

The impact data recorded for the z axis was plotted against time. The plot is shown in fig 16. It can be deduced from fig 16 that the highest impact g-force in the vertical direction was experienced between 458 seconds and 482 seconds since the start of the data recording. The maximum g force experienced in the z direction was 4.18g (positive, thus experienced impact from the top).

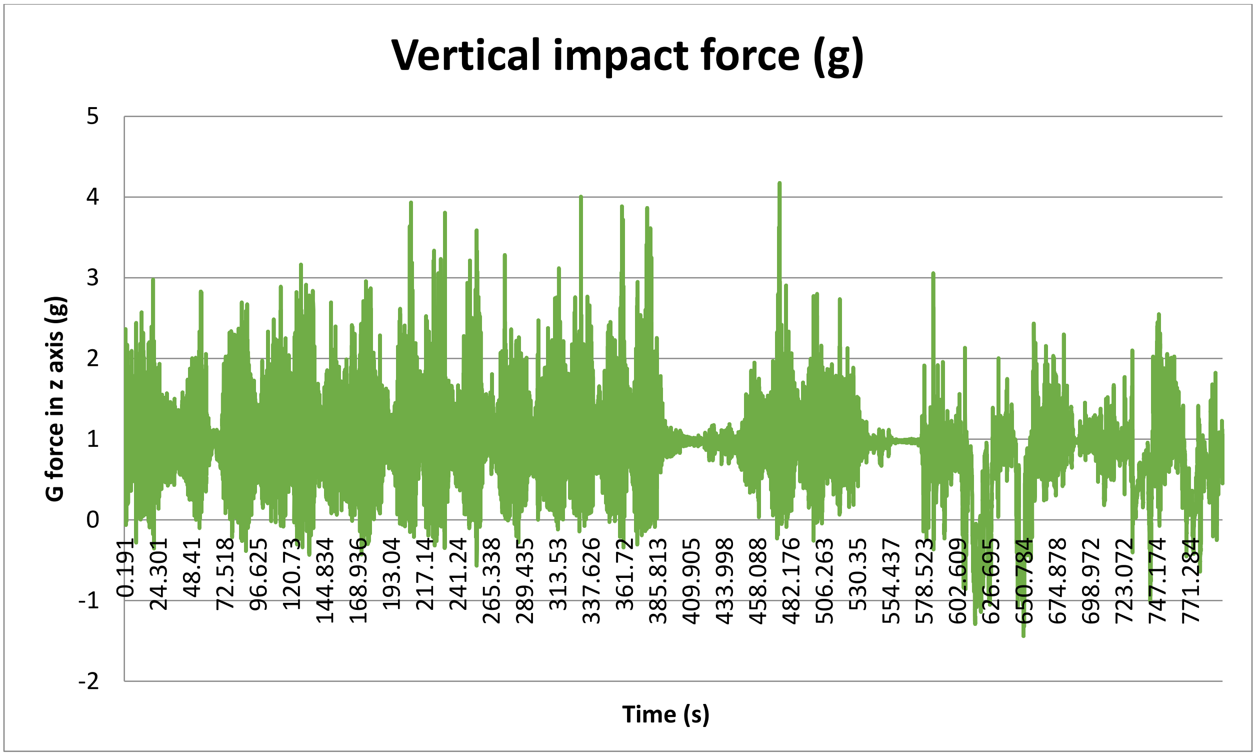

Figure 16 G-force recorded in the z axis

From fig 16, it can also be seen that an impact force of -1.44g was experienced by the Jet Ski between 636 seconds and 674 seconds. This is a negative g force, thus it was experienced from the bottom face of the Jet Ski.

Similarly the impact force recorded in the x axis is shown in fig 17

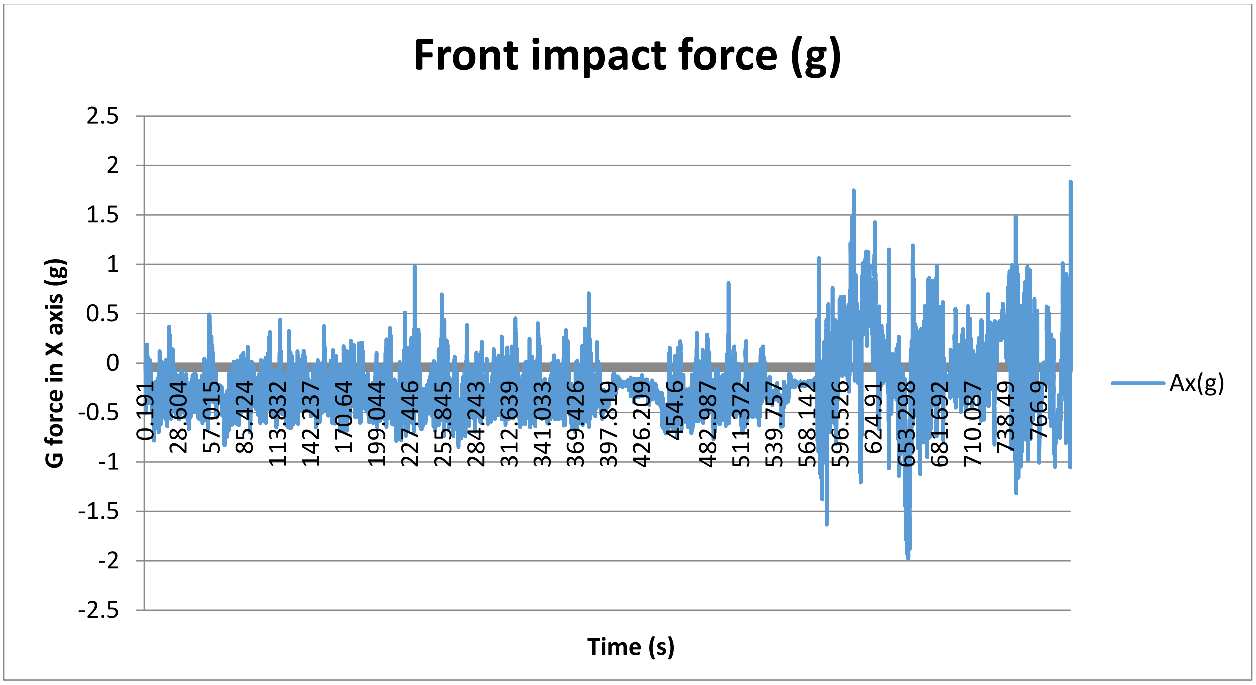

Figure 17 G-force recorded in the x axis

From the fig 17, it can be deduced that the highest impact force experienced in the x axis occurs between 624 seconds and 655 seconds. The maximum impact force was recorded as -2g. This is a negative g force, thus the impact occurred from the rear of the Jet Ski. The accelerometer also recorded a positive g force of 1.83g. This impact was recorded between 800 seconds to 850 seconds. This impact was registered as a positive g force impact, thus the impact occurred from the front of the Jet Ski. .

Lastly the impact force recorded for the y axis is shown in fig 18. As seen in fig 18, the maximum impact force experienced in the y direction was -2.63g and it occurred between 466 seconds to 493 seconds. This was a negative g force, thus the impact force was experienced from left hand side of the Jet Ski. The accelerometer also recorded a 2.21 g force between 658 seconds to 685 seconds. This impact was registered as a positive impact, thus the impact occurred from the right hand side of the Jet Ski.

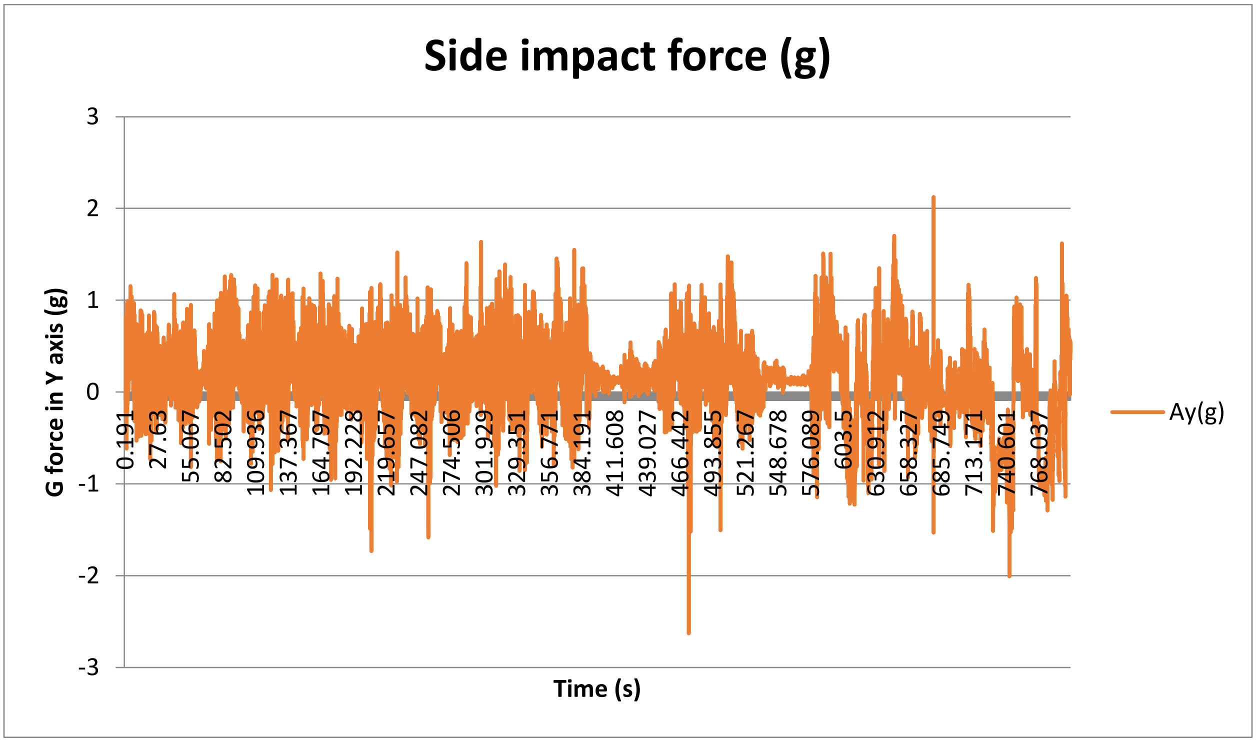

Figure 18 G-force recorded in the y axis

4.4.2 Discussion

The obtained data from the accelerometer revealed that the maximum g force experienced by the Jet Ski is -2g, -2.63g and 4.18g for the x, y and z direction respectively. The NCOP14 impact standards (outlined in table 1) states that the a battery restraining system must withstand an impact of 20g for front impact (i.e. x direction), 15g side impact (i.e. y direction) and 10g vertical impact (i.e. z direction). Due to the large difference between the recorded data and the standard, the REV Jet ski team concluded that using the NCOP14 standards for the design of the battery restraining system was inappropriate. The design of the battery restraining system will now be guided by the data obtained from the accelerometer experiment.

The X16-1C accelerometer has been stated to have an error of 5%-10% from the recorded data (Gulf Coast Data Concepts 2007). Thus, before using the data obtained for stress analysis, a decision was made to apply a safety factor of 1.5. This would account for accelerometer error and environmental factors. Thus the final design of the battery restraining system and the motor mounting system will be governed by the following impact requirements.

Table 2 Impact requirement for the battery restraining system and the motor mounting system

Impact direction	Requirement
A_x	$-2 \times 1.5 = -3g$
A_y	$-2.63 \times 1.5 = -4g$
A_z	$4.175 \times 1.5 = 6.3g$

5. Battery Restraint System Design for the Jet Ski

5.1 Overview

The REV Jet Ski shown in fig 3 must house large quantities of lithium based batteries in order to deliver sufficient energy for the 50kW, 96V motor. The battery restraining system, which house the lithium ion batteries must be designed in accordance to relevant standards and regulations. It must also be able to withstand forces that the Jet Ski is likely to experience in extreme operating conditions. This specific chapter will detail the requirements and the design process followed for the development of the battery restraining system.

5.2 Design Process

5.2.1 Battery Restraining System Design Requirements

The design requirements for the battery restraining system is outlined below.

1. The REV Jet Ski must be able to supply a current of approximately 500A to a 96V motor. Thus to have a satisfactory run time, the REV Jet Ski must house 140 lithium ion batteries, each producing a potential of 3.2V. Initially, having fewer than 140 batteries were considered, however this would significantly reduce the run time or the power output of the Jet Ski.
2. The battery restraining system must have easy access to the housed batteries. This consideration was provided so that failing battery cells could be easily accessed and replaced. A consideration was also given for the battery cage to be fabricated in a manner which would allow further modifications and alteration in the future.
3. The battery modules must be held tight in place. However there must be at least 20mm of clearance on the top of the battery modules to allow space for the battery management system and the connections between the modules.

4. The battery restraining system must be placed in a position where it can achieve a similar weight distribution to the original Jet Ski, and built to achieve a similar weight distribution.

5.2.2 Constraints

Outlined below are the constraints which guide the design of the battery restraining system.

1. As mentioned in section 4.5 (discussion of the impact data obtained from the experiment), applying impact requirement outlined in the NCOP14 standard to the battery restraining system of the Jet Ski was not appropriate. The impact requirement outlined in NCOP14 stipulates that a battery restraining system must withstand an impact force of 20g front impact, 15g side impact and 10g rear impact. However, the impact data obtained from the experiment (see section 4) indicates that at peak performance, the Jet Ski experiences a front impact of 1.83g, vertical impact of 4.175g, and side impact of 2.68g. Since the device used to record the impact data is prone to an error of 5 to 10 percent, a safety factor of 1.5 was applied. Thus the battery restraining system will now be required to withstand 2.7g front impact, 6.3g vertical impact, 4g side impact.
2. A critical determinant for the design of the battery restraining system is available space within the Jet Ski after removing the internal combustion engine component. The petrol engine motor located in the aft section of the Jet Ski was planned to be replaced with an electric motor of similar performance and the fuel tank located in the front section of the Jet Ski was planned to be replaced by the battery restraining system. The aft section of the Jet Ski will house most of the electrical components (i.e. controller, converter, cooling system), electric motor and the motor mounting system. The front section of the Jet Ski would contain all of the batteries and the battery restraining system. This placement was hoped to preserve the weight distribution of the Jet Ski and have a front to aft weight ratio if 50:50.
3. The REV Jet Ski is attempting to replicate the performance of the original Jet Ski, thus the hull, steering system and the propulsion method of the Jet Ski must remain unmodified.
4. When selecting an appropriate placement for the battery restraining system, it is important to consider the Jet Ski structure adjacent, to mount the batteries. Thus existing mounting points and bolt holes were used before other methods were considered.

5. The battery restraining system must be completed by a reasonably low cost to the REV program. Priority was placed to make the design as simple as possible, thus lowering the time taken to fabricate the battery restraining system.

5.2.3 Battery Specification

5.2.3.1 Initial proposal

As a power source for the Jet Ski motor and the electrical system, lithium ion sulfate batteries by thunder sky, model TS-LFP100AHA was initially considered. This battery has a nominal voltage of 3.2V, and they are individually sealed. The TS-LFP100AHA batteries weigh 4.5kg each and the batteries are to be stored upright or flat on the largest face (ThunderSky 2007). The dimensions for this battery are shown in fig 19.

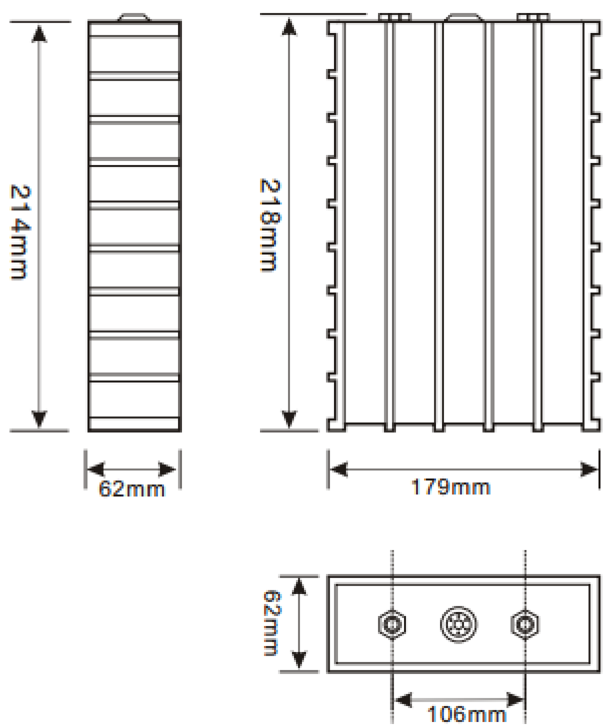

Figure 19 ThunderSky TS-LFP100AHA

Initially, a battery restraining system was designed for the TS-LFP100AHA batteries. However it was found that the delivery of this type of battery had a lead time of 13 weeks. Due to sever time constraints the TS-LFP100AHA was abandoned for batteries with shorter delivery lead time and lower cost.

5.2.3.2 Final proposal

Due to the unavailability of TS-LFP100AHA, another energy source for the REV Jet Ski was investigated. After an extensive investigation, the Headway 10Ah batteries were considered. The batter headway battery and the specifications are listed in fig 20 and table 3.

Figure 20 Headway 10Ah

Table 3 Headway 10Ah batteries

Chemistry	Lithium Iron Phosphate
Dimension (mm)	Length 120mm, Diameter,
Nominal Voltage (V)	3.2V

The headway 10Ah batteries were relatively low cost and it was immediately available from EV works (suppliers of electric vehicle components).

The electrical engineering members of the REV Jet Ski team proposed to connect 8 batteries in series to produce 80Ah battery modules. The Modules will be treated as a cell. A completed battery module is shown in fig 21.

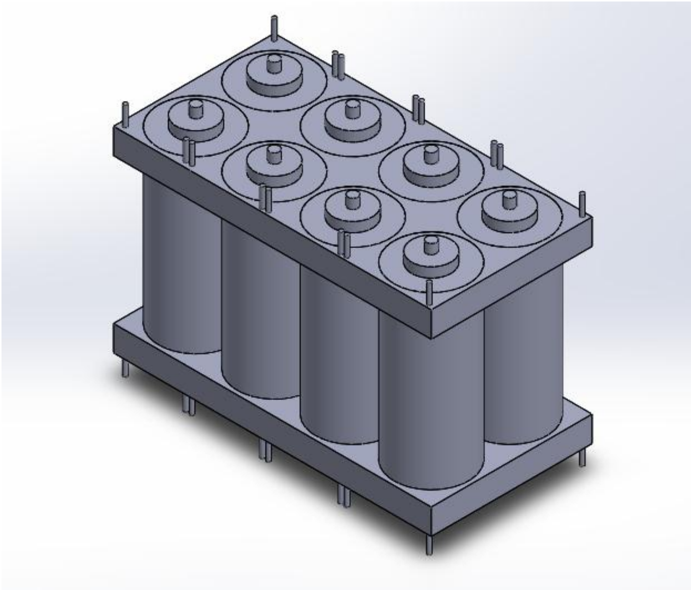

Figure 21 Battery Module

The batteries within the module are held together tightly by plastic connectors. The headway modules are also recommended to be held upright or flat on the largest face. Each battery module was weighed and found to have mass of 2.64kg. The dimensions of the modules are shown in fig 22.

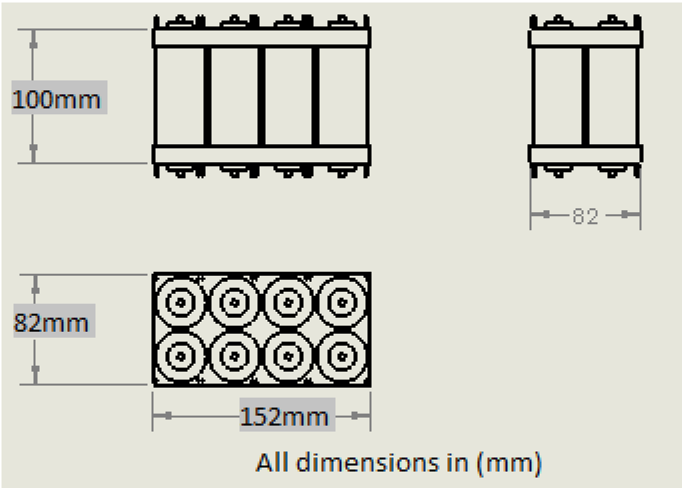

Figure 22 Dimensions for the battery module

5.2.4 Design Software

Preliminary concepts and the final designs for the battery restraining system was undertaken using the 3D design software SolidWorks. This software is a powerful design tool which allows the user to create and modify complex designs. When the design of the battery restraining system was completed using SolidWorks, the design was imported in to ANSYS workbench to perform a stress analysis. In order to import a Solid Works file, the file must be saved with an IGS extension and later imported into ANSYS workbench using the Import geometry feature. Thus if the designs did not pass the stress analysis in ANSYS Workbench, they were easily modifiable through SolidWorks and imported back to ANSYS Workbench.

5.2.5 Design Methodology

The steps and processes followed for the design of the battery restraining system is shown in the flow chart in fig 23. The first step in the design processes was to identify the constraints that are governing the design of the battery restraining system. Once the constraints and requirements are identified, conceptual designs were developed. The concept designs were presented to the REV Jet Ski team members and the supervisor for discussion. If the designs were approved by the supervisor, the designs were computerized on the SolidWorks design software. Subsequently, the SolidWorks designs were presented to the mechanical engineering workshop and the physics workshop to discuss the feasibility and the cost involved for the design to be fabricated. This was an important steps as some designs were rejected due to its complexity and high cost of fabrication. If the design was deemed too expensive of complex, members of the staff in the physics workshop and the mechanical work shop was able to advice on necessary modification and simplification which would lead to lower the cost of fabrication and labor.

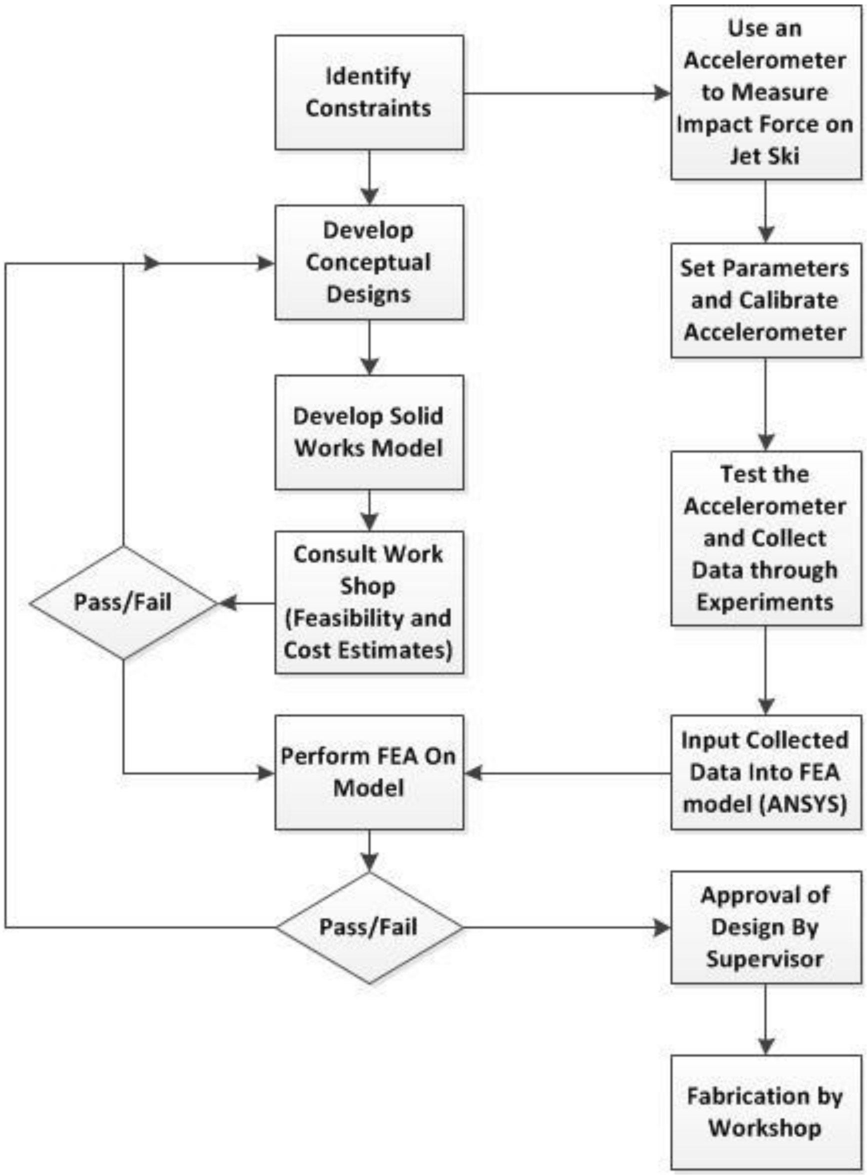

Figure 23 Design flow chart

If the fabrication cost of the design estimated by the workshop was deemed acceptable the design will then undergo a stress analysis using ANSYS workbench. The stress analysis will confirm if the design will be able to withstand impact requirements outlined in section 4.4.2. In order to obtain accurate results, each mesh for the components were refined to obtain a maximum von-mises stress which converged within 5%. If the stress analysis did not yield acceptable results, the designs were modified until a satisfactory stress analysis results are obtained. Once all the designs were completed. They were approved by designated REV supervisors for construction by the workshop.

5.2.5 Safety

As mentioned in section 5.2.2, constraint 1, the design of the battery restraining system was governed by the safety requirements obtained through impact experiment (shown in section 4). NCOP14 standards were followed for miscellaneous design requirements such as venting of the batter compartment and labelling of high voltage components. Another safety aspect considered was the safety requirement during fabrication and installation within the workshop.

5.2.5.1 Design safety requirement

The design of the battery restraining system is governed by safety requirements. The system is designed in a manner which restraints the batteries during peak operation of the Jet Ski. The safety requirements have been outlined within section 5.2.2 and section 4.5. It will be further discussed in the results section.

5.2.5.2 Fabrication and installation safety requirement

The final design of the battery restraining system contained 21 different components. The physics workshop and the mechanical workshop was required to fabricate 12 components, and 9 components were purchased or fabricated by 3rd party workshops. Once the components were fabricated, the assembly of the components were intended to be carried out in the G.50 REV laboratory located on the ground floor of the Electrical Engineering Building. The G.50 Lab contains the REV vehicles and basic tools such as heat guns, drilling equipment and sanding machines. For complex fabrication process, mechanical workshop and physics work shop was utilized.

To utilize the G.50 laboratory, a safety induction was performed with an emphasis on the following key areas.

- Keep the laboratory clean and free of obstacles that may cause a fall.
- Covered shoes must be worn during the time spent inside the G.50 laboratory.
- Long hair must be tied back.
- PPE such as safety glasses, ear protection, and gloves must be worn when appropriate.
- Foods and beverages are not allowed within the confines of the laboratory.
- Smoking is not allowed within the laboratory.
- The emergency number is 2222 from the UWA telephones or 6488 2222 from any telephone.
- When lifting heavy equipment, bend your knees and lift using your legs. If the equipment is too heavy ask for assistance from other members within the lab (UWA Safety & Health Manager 2007).
- High voltage equipment used within the lab should not be touched without a qualified electrician.
- In case of a fire, activate the nearest fire alarm and proceed to evacuation area.

- In case of an evacuation, the evacuation area for all personnel within the G.50 lab is located in the electrical engineering court yard.
- Seal and mark all electrical equipment in the G.50 Laboratory as instructed by the relevant standard and regulation.
- If a person experiences an electric shock, medical advice must be obtained even as a precaution. The WA Electrical Regulation requires all electrical accidents be reported.
- Any an injury occurs within the laboratory, medical advice must be sought and the UWA technical officer or UWA electrical supervisor must be informed of the incident. An incident report form must also be filled.
- Report all hazards and unsafe conditions

The mechanical workshop and the physics workshop have its own safety regulations. The list of requirements and regulations can be found from the UWA website (UWA Occupational therapist 2001). In workshop regulations, above mentioned requirements and some additional requirements are present. The additional requirements are shown below.

- PPE must be worn at all times
- Students must be accompanied by a workshop staff member to operate equipment within the workshop.
- Approval must be sought to access all equipment within the workshop.
- Machines must be used for their intended purpose.

All of the above safety regulations were enforced during the fabrication process and they will be enforced during the assembly process.

5.3 Results and Discussion

5.3.1 Battery restraining system location and battery arrangement

As discussed in section 3.1, there are 5 possible mounting points which could be used for the mounting of the battery restraining system. However the mounting points located in the aft section of the Jet Ski could not be used as it was intended for the AC motor and the motor mounting system. Thus the only possible mounting points that could be used to restrain the batteries were mounting point 1, 2, and 3 located in the front section of the Jet Ski. This section also had adequate space to house the required amount of batteries.

The battery box designed to house the battery modules will be mounted on a supporting frame Appendix C. Supporting frame was created to connect mounting point 1, 2, and 3 and distribute the load of the battery box to each of the mounting points. It also allows the battery

The front section of the Jet Ski intended to house the batteries, previously contained a 60 L fuel tank in the original version of the Jet Ski. The front section of the Jet Ski is shown in fig 4. In order to preserve the weight distribution of the Jet Ski, every attempt was made to place the batteries within the space previously occupied by the fuel tank. This meant that the battery modules had to be stacked in 3 layers, each layer, containing 10 battery modules. The battery arrangement of layer 1 is shown in fig 24

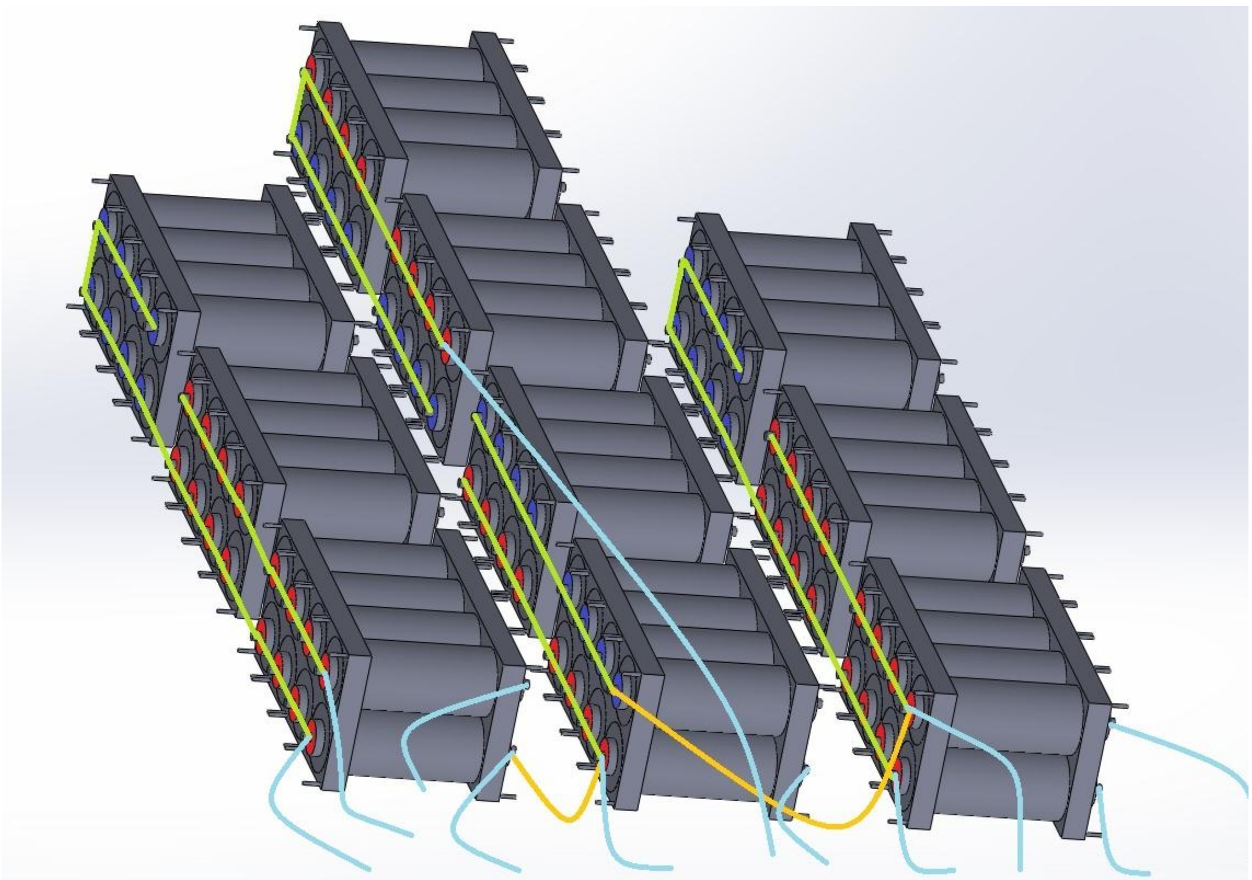

Figure 24 Initial battery module arrangement

This configuration was later changed to 3 layers with the first layer containing 12 modules, the second layer containing 9 modules and the third layer containing a further 9 modules, making a total of 30 modules of batteries powering the Jet Ski. This configuration for layer 1 is shown in fig 25 and the configuration for layer 2 and 3 is shown in fig 26. This change was made due to high cost estimate for fabrication for the design which accommodated the 10 battery modules in each layer. This issue is discussed in the following section in detail.

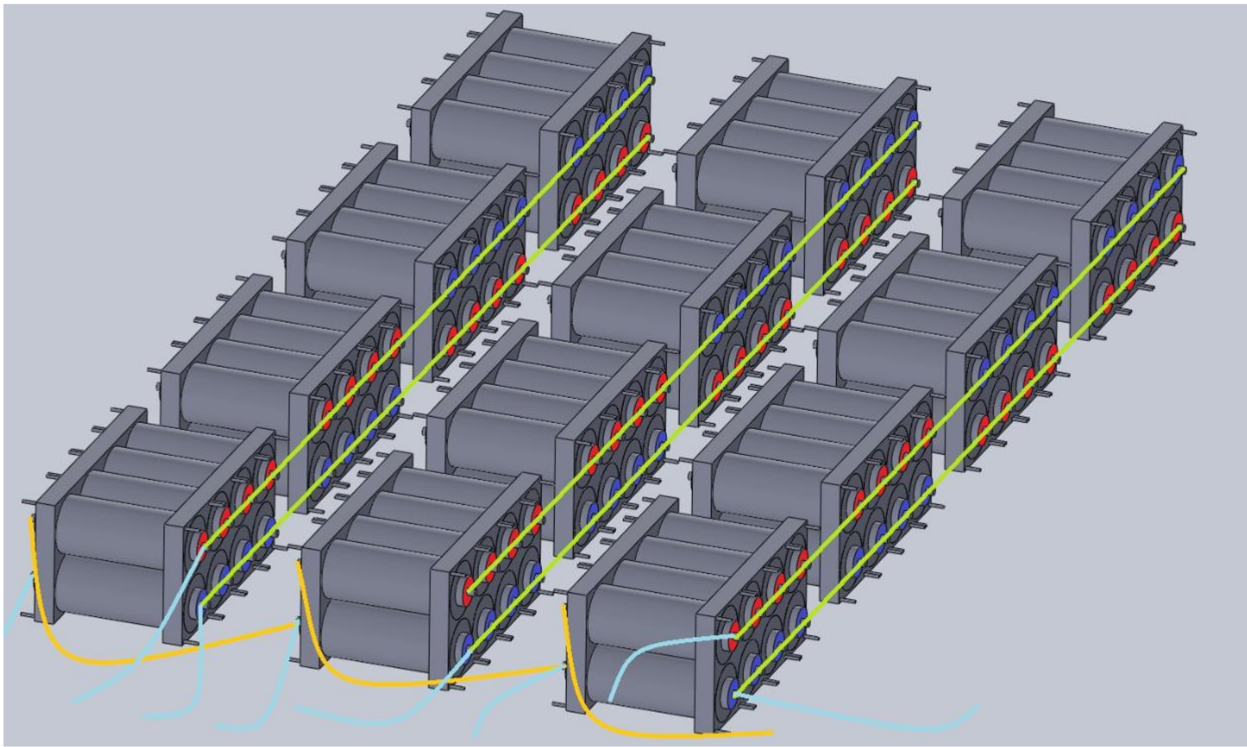

Figure 25 Revised configuration for layer 1

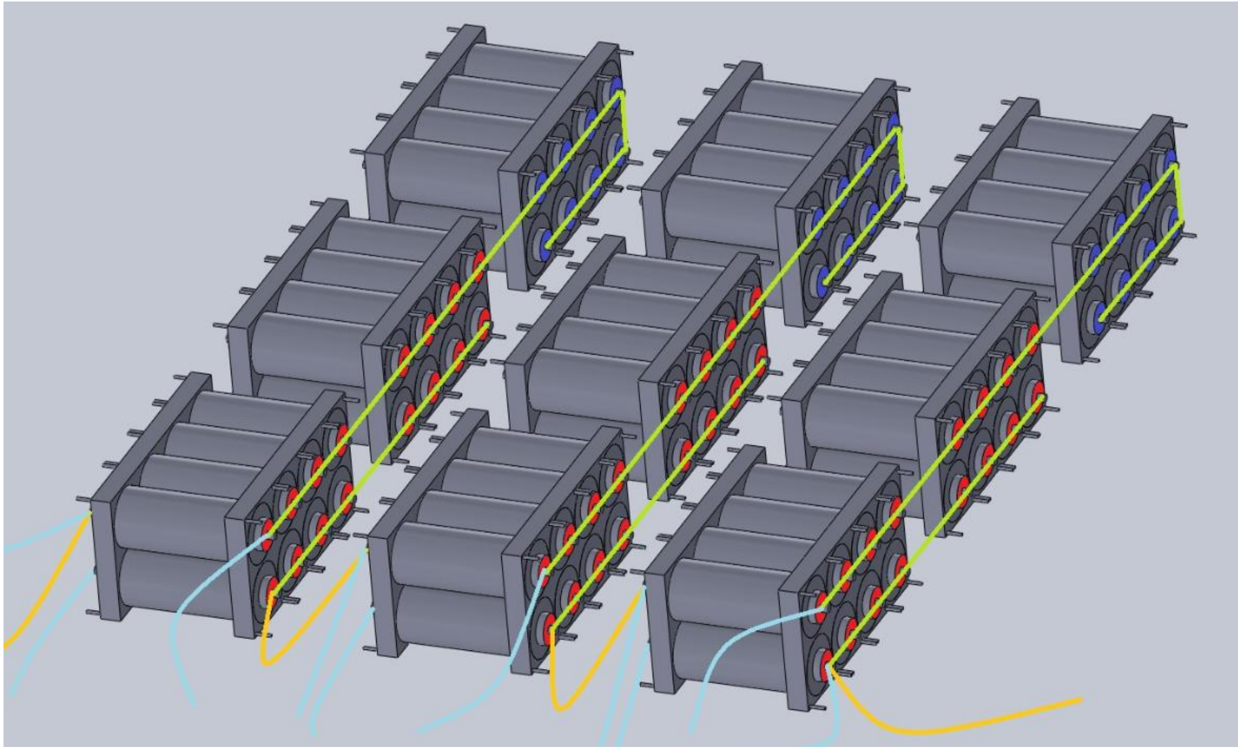

Figure 26 Revised configuration for layer 2 and layer 3

5.3.2 Material Selection

Suitable material for the construction of the battery restraining system must meet the following key requirements.

- Low cost.
- Light weight.
- High yield strength.
- Easily modifiable for changes at later stage.
- A common material that is readily available from the workshop.
- High corrosion resistance

Aluminum alloy (6060/T5) and Mild Steel (AS3679.1) were chosen as they closely matches the requirements outlined above. Main differences between the two materials were density and strength. The material properties for the two materials are shown in table (). Preliminary stress analysis showed that for the impact requirements outlined in section 4.5, the strength of the aluminum alloy was sufficient. Although mild steel has greater values for both yield strength and tensile strength, it was it was approximately 3 times heavier. Thus using steel to fabricate the battery restraining system was abandoned as it was believed that the extra weight would be detrimental to the weight distribution and the performance of the Jet Ski. In conclusion, Aluminum alloy was used to fabricate the battery restraining system. The figures from the table are taken from Standards Australia 1997.

Table 4 Material properties from Standards Australia 1997

	Aluminum Alloy (6060/T5)	Steel (AS3679.1)
Density	$2700kg/m^3$	$8050kg/m^3$
Minimum Yield Strength	$110MPa$ (0.2% $proof\ stress$	$320MPa$
Minimum Tensile Strength	$150MPa$	$440MPa$

5.3.3 Battery box design

The design of the battery box must focus on restraining the batteries during peak operation and in collision. The battery box must be able to withstand g forces outlined in section 4.4.2. The battery box must be designed so that the fabrication and assembly cost could be minimized. Within the battery box, there must be sufficient clearance for high current cables and wires. Other considerations for the designs are shown in section 5.2.2. Designs were produced and modified until the goals mentioned above were satisfied.

5.3.3.1 Initial design

Figure 27 shows the initial design proposal for the battery box. This system employs the battery arrangement method shown in fig 24 of section 5.3.1 where the battery modules are arranged in 3 layers with each layer containing 10 battery modules. This battery box design was proposed to be made from 5mm thick Aluminum alloy sheets. Each layer was deliberately designed with 5mm clearances on all sides which would accommodate thermal expansion from the battery modules. 20mm clearance was given from the battery modules to the top section in each layer. This clearance was provided to install the BMS and allow room for electrical wires. An exploded view of this battery box can be seen from figure 28.

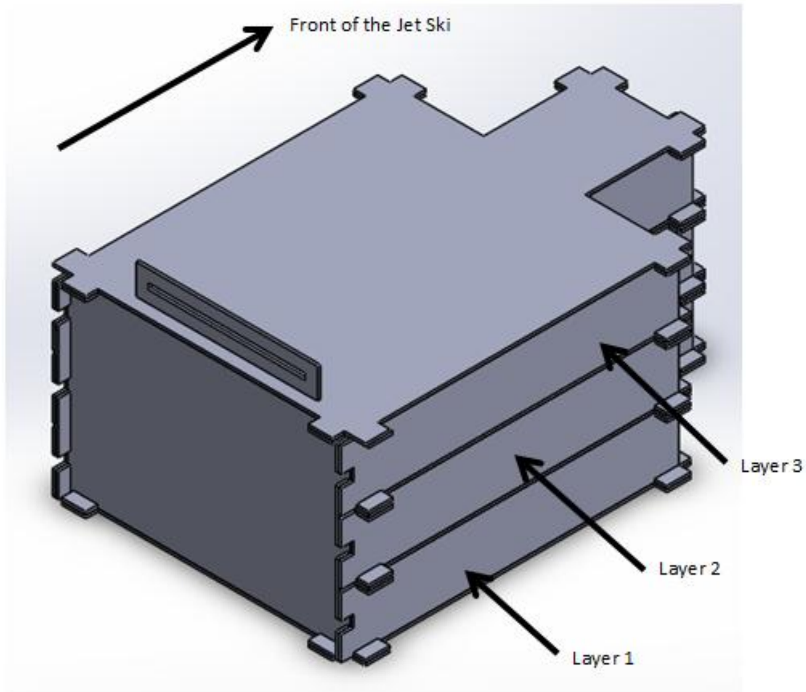

Figure 27 initial design proposal

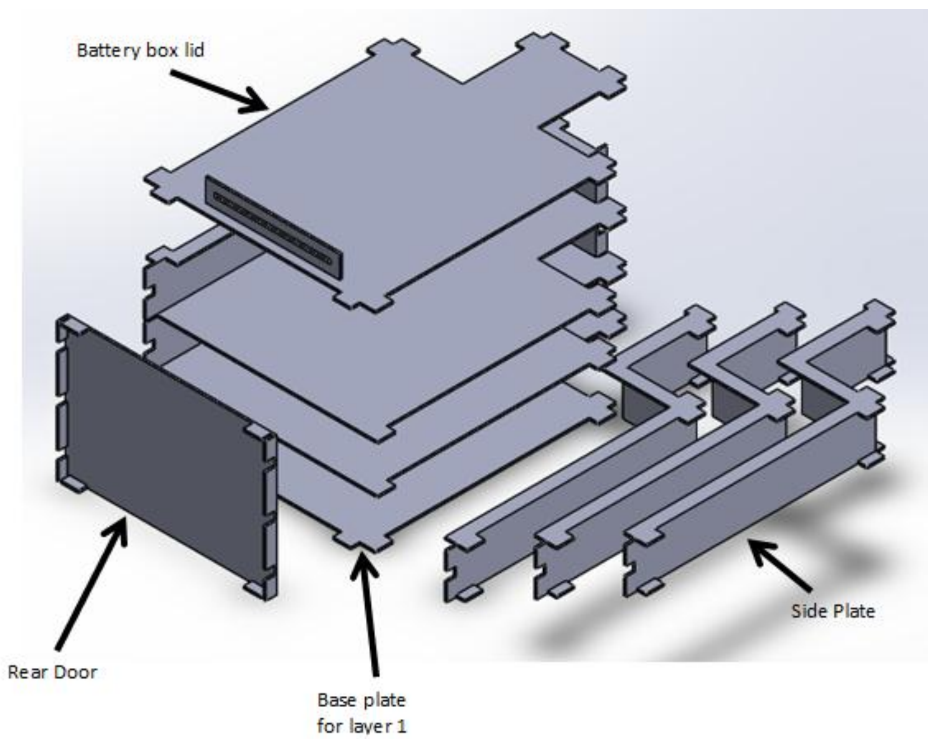

Figure 28 Exploded view of the initial design

The exploded view (figure 28) shows the various components used to assemble the battery box. As mentioned earlier, all of the components are fabricated using 5mm Aluminum sheets.

Aluminum blocks measuring 25mm width, 30mm length and 5mm height are attached to each of the component through welding. When the battery box is assembled, all of the components were intended to be bolted on through the Aluminum blocks.

The initial design shown in figure 27 and figure 28 was rejected upon the feasibility and cost estimate stage of the design process see figure 23. The mechanical engineering workshop was reached for to conduct the feasibility study and to obtain a cost estimate. The staff at the workshop advised that his design is too complex to be fabricated in a timely fashion. This design required the welding of small Aluminum blocks to components such as the rear door, side plates and base plates. This would require welding of the Aluminum block in 56 different places within the battery box. Since Aluminum welding is exceptionally difficult (due to high thermal conductivity and high thermal expansion coefficient) the task of fabricating the battery box would be time consuming and costly (Jones, D 1996).

5.3.3.2 Final design

Figure 29 shows the final battery box design. This battery box focused heavily on lowering the number of components used to lower the cost of fabrication and assembly. This battery box design is also intended to use Aluminum components for the assembly however, unlike the previous designs the final battery box design does not have any welded assemblies. This battery box was also designed to have a clearance of 5mm on the left, right and forward section of the battery modules. The battery box also allows 20mm clearance between the battery modules and the roof of each of the layers.

This battery box is designed to accommodate the battery arrangement shown in fig 25. This configuration is intended to have 12 battery modules in layer 1 and 9 battery modules in layer 2 and layer 3.The exploded view of this battery box is shown in fig 30.

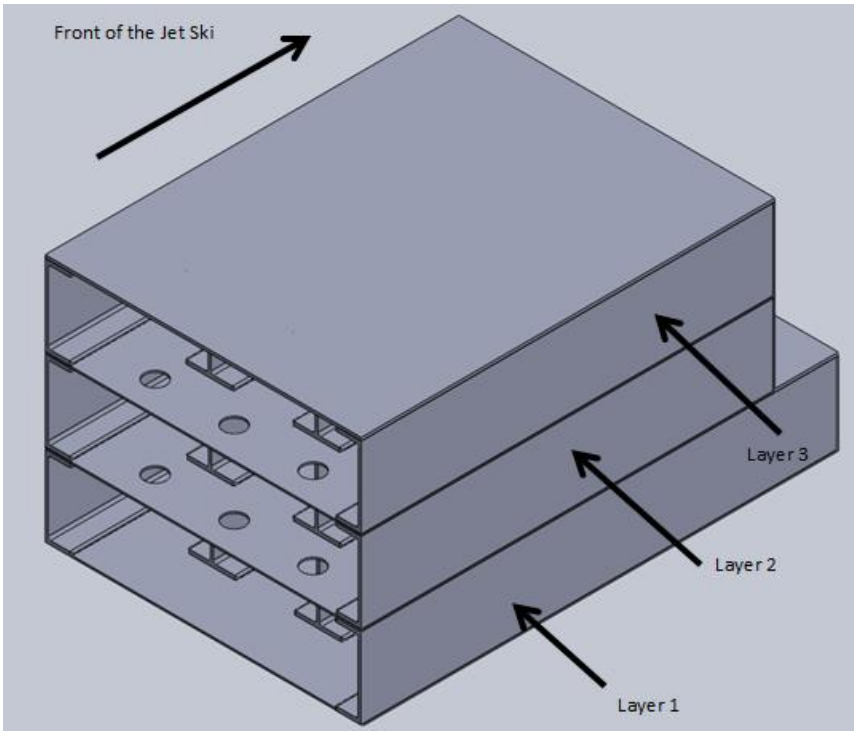

Figure 29 Final Design

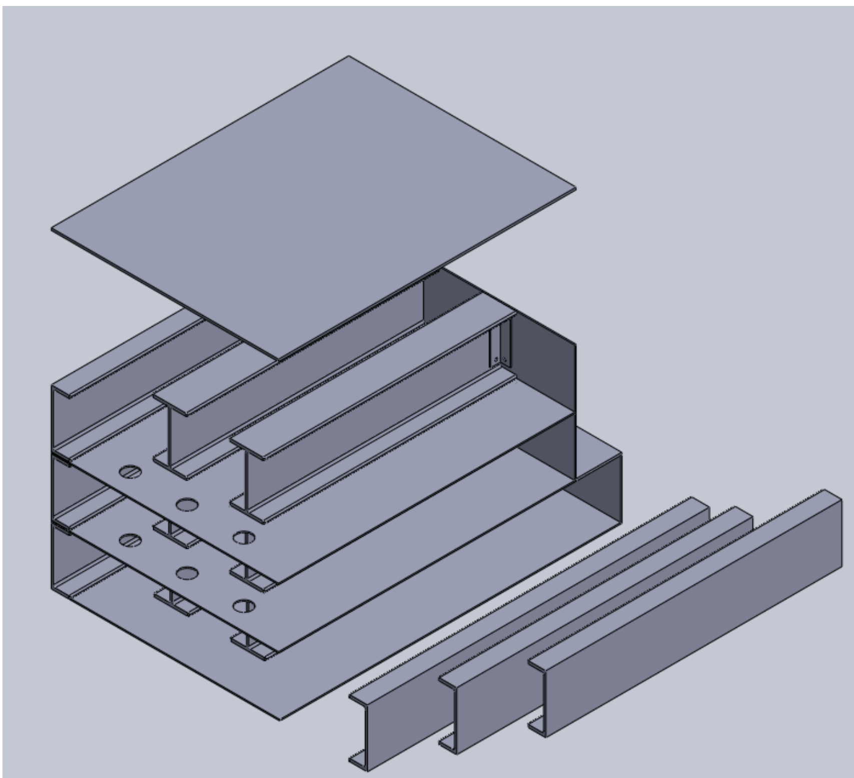

Figure 30 Exploded view of the final design

As seen from the exploded view of the battery box (see figure 30), each layer of the battery box is supported by 2 Aluminum I-beams and 2 channel beams. I-beams are used to support the weight of the batteries and the weight of the battery box assembly layer located immediately above. The Aluminum I-beams are also used to separate one row of battery modules to another which will prevent the excessive movement of the battery modules within the battery box layer. The I beam profile used for this battery box is shown in fig 31

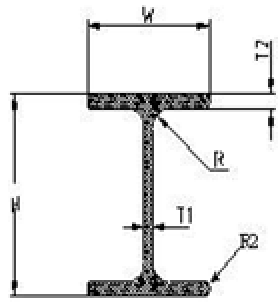

Height (mm)	Width (mm)	T1 (mm)	T2 (mm)	R (mm)	R2 (mm)	Length (m)	kg/m
130	80	4.8	6.35	4	3.175	6.5	27.521

Figure 31 Aluminum I-beam profile (One Steel 2013)

As seen on figure 30 a 100mm clearance was provided between the I-beams and the rear of the battery box. This clearance was used for electrical wiring between the 3 rows of battery modules. On the base plate of layer 2 and layer 3, a 35mm diameter hole was cut to let large electrical cable to connect battery modules between 2 layers of the battery box.

As seen on fig 30, Channel beams were used as the side support for each layer of the battery box. The Channel beams were fabricated by sawing off one side of the flange of the I-beam. The Channel beams were used as to restraint the battery module, support the weight of the modules as well as the battery box layer located immediately above.

Within the battery box, the I-beams and Channel beams are bonded through the use of 3M structural double sided adhesive tape. This type if adhesive tapes are becoming widely popular in the construction industry as a replacement for bolts and rivets. The particular double sided adhesive tape intended to be used for the battery box is 3M 4941 VBH tape, which is categorized as one of the strongest adhesive tapes offered through 3M. The normal tensile performance and the dynamic shear overlap performance of the 4941 tapes are 690kPa and 550kPa respectively.

This value will be taken into consideration during the stress analysis process. Further information on the 3M adhesive tapes can be found in Appendix D.

To prevent the shorting of batteries, 1mm thick polycarbonate sheets were placed between the channels, base plate and the I-beam for each of the rows. The polycarbonate sheets are also excellent insulators (Dotmar 2012), thus it will keep the temperature of the battery box relatively even during peak performance.

A method to restraining the batteries from the rear of the batter box is still being considered. A bolt on aluminum sheet is currently being considered as a possible method for restraining the batteries from the rear section of the battery box. This method requires further discussions with the supervisor, REV Jet Ski team and the workshops. Once a method is devised, a stress analysis can be conducted on the viability of the method.

5.3.4 Stress Analysis.

A stress analysis must now be conducted on the final design of the battery box. The stress analysis is carried out by the ANSYS Workbench software. As outlined in section 4.5, the battery restraining system must be able to withstand 2.74g front impact, 3.94g side impact and 6.26g of vertical impact. The surfaces of battery box where the adhesive tapes are applied were checked for their adherence to these forces.

The Solid Works model developed for the final design of the battery box can be imported into ANSYS workbench for the stress analysis. Appropriate supports and pressures are applied to each layer of the battery box, and a simulation is conducted to obtain the safety factor for the maximum equivalent stress (Von-Mises Stress) against the yield strength of the material. Each battery box layer was designed to a minimum safety factor of 1. This was due to the safety factor of 1.5 that was applied to the impact g-forces in section 4.5. The maximum Von Mises stress was converged to within 5% through refining the mesh.

5.3.4.1 Applied pressure on the battery box.

Since the battery box layers are stacked on top of one another, the required pressure that each layer must withstand can vary. This is also due to the difference in the size of battery box layer 1 from layer 2 and layer 3. The required pressure the battery box layer must with stand can be calculated by required acceleration times the total mass of the batteries and the mass of the battery box layers located above. This value must then be divided by the surface area where the pressure is applied. An example calculation for the case for a side impact on battery box layer 1 is shown below. And the required pressure for each layer is summarized in table ().

$$F_{side\ impact} = 3.94 \times 9.81 \times m \quad (1.1)$$
$$Where\ m = 104kg$$
$$F_{side\ impact} = 3.94 \times 9.81 \times 104 = 4.02 \times 10^3 N$$
$$A_{channelbeam} = 1.04 \times 10^{-1} m^2$$
$$\frac{F}{A} = \frac{4.02 \times 10^3}{1.04 \times 10^{-1}} = 3.93 \times 10^4 Pa \quad (1.2)$$

Table 5 Required Pressure

		Battery Layer 1	Battery Layer 2	Battery Layer 3
Pressure (Pa)	**Front Impact**	**40611**	**23256**	**9278**
	Side Impact	**39314**	**25484**	**10173**
	Vertical Impact	**36331**	**24235**	**9474**

As seen from table () pressures applied on the surface are much lower than the nominal tensile performance and dynamic shear overlap performance of 650kPa and 550kPa. Thus the adhesive tapes are a suitable method to restrain the I-beams and channel beams to the base plate. For this reason, contacts between 2 faces facilitated through the use of adhesive tapes are assumed to be fixed supports.

When conducting the stress analysis the required pressure was assumed to be evenly distributed along the surface area. The stress analysis for each battery layer will be conducted in section 5.3.5.

5.3.4.2 Analysis refinement

When conducting the stress analysis through ANSYS workbench, the convergence feature was used to refine the mesh until the maximum equivalent stress converged within 5%. Convergence is achieved through increasing the fineness of the mesh by increasing the number of nodes and elements as well as decreasing the size of the elements (Logan, D 2012). The mesh fineness of improved automatically through the convergence feature in ANSYS Workbench.

5.3.5 Finite element analysis of the battery box

5.3.5.1 Battery box Layer 1

The stress analysis of layer 1 of the battery box is conducted through the use of ANSYS Workbench. Analysis for the front Impact, side impact and vertical impact will be undertaken. The results are shown in the following sections.

5.3.5.1.1 Front Impact

After the finite element analysis the maximum deformation and the minimum safety factor is calculated. The pressure applied to the front face of the battery box layer 1 can be found in table 5. The FEA analysis results for total deformation and safety factor is shown in fig 32 and fig 33 respectively. The battery layer 1 performed above the required standard for the impact acceleration condition of 2.74g in both total deformation and safety factor requirement. The total deformation for this impact condition was found to be 0.182mm located in the center of the front plate with a safety factor greater than 1. The minimum safety factor was found to be 1.579, located on the right hand side of the front plate. This result indicates that the battery box layer 1 is able to withstand a front impact pressure of 40611Pa.

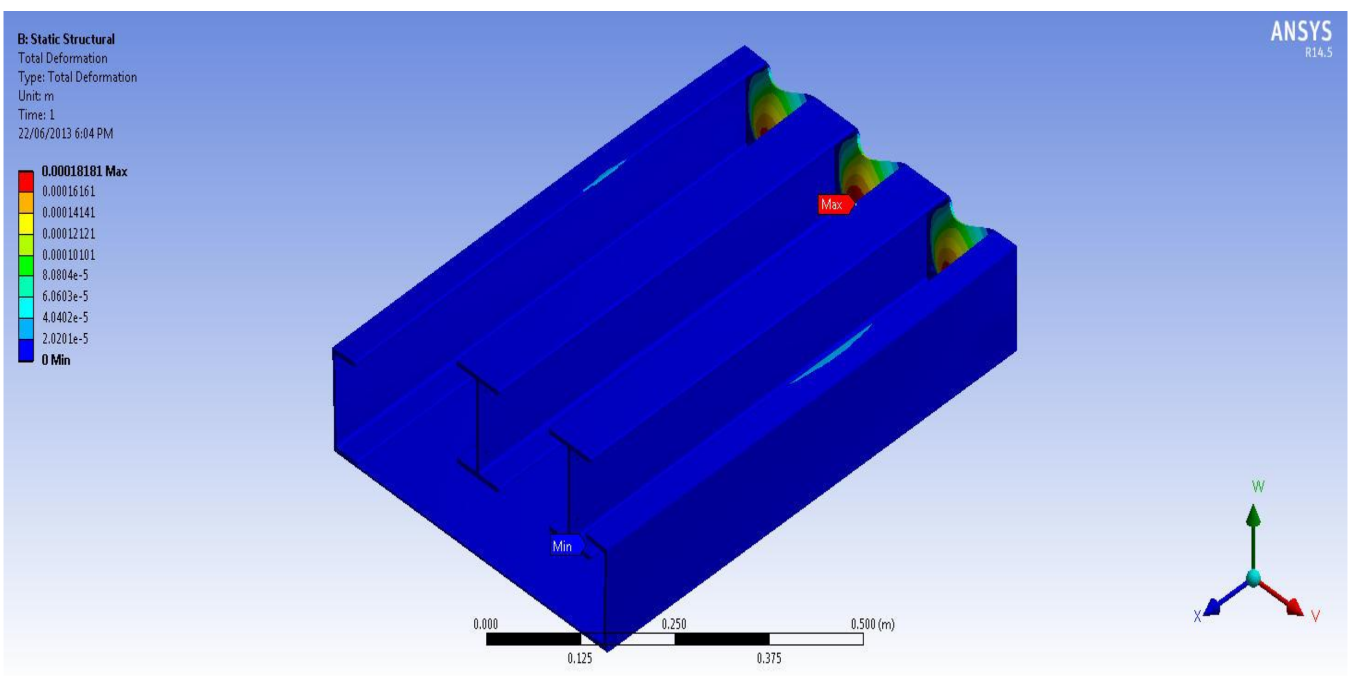

Figure 32 Total deformation, front impact, layer 1

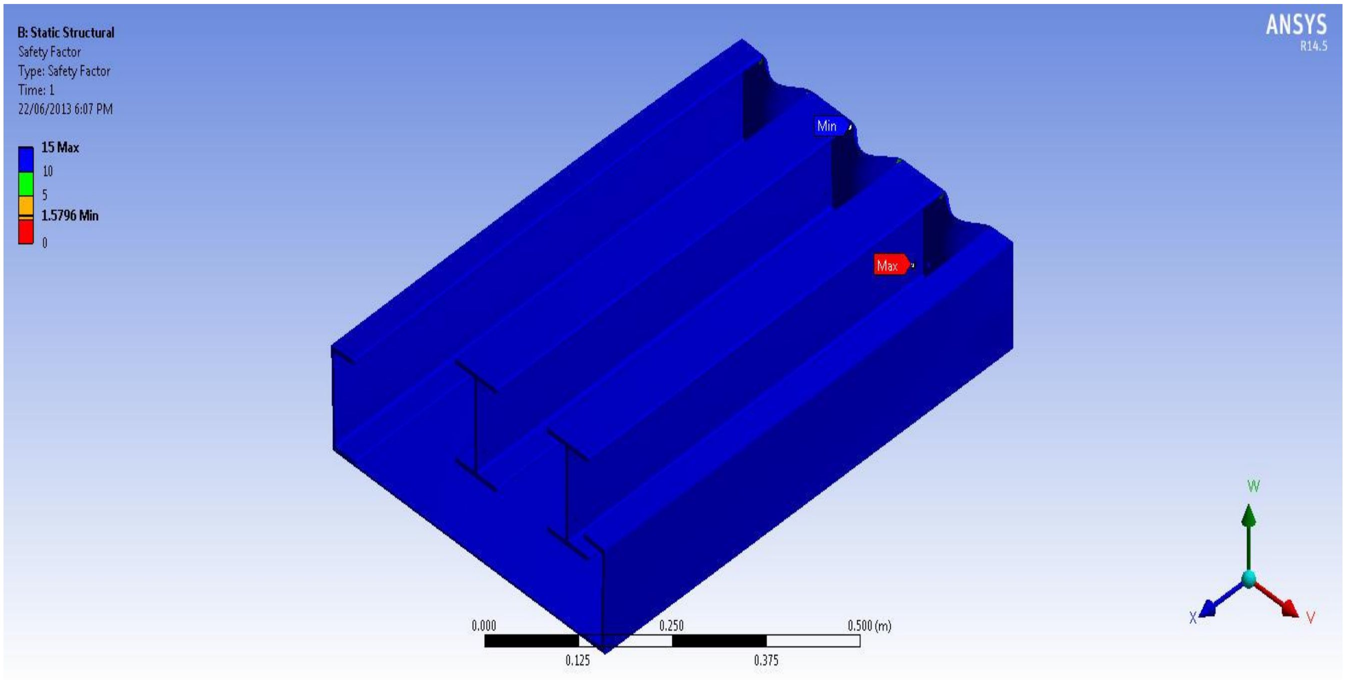

Figure 33 safety factor, front impact, layer 1

5.3.5.1.2 Side Impact

The battery layer 1 is designed symmetrically along the centerline of the battery box, thus the geometry of the left hand side and the left hand side of the battery box layer 1 is identical. Thus it can be concluded that theoretically an impact on the left hand side would yield identical results to a pressure applied on the right hand side, given an identical pressure is applied. Due to this reason the stress analysis was only conducted on the left hand side of battery layer 1.

In this simulation a pressure of 39314Pa is applied to the right hand side layer 1. The analysis results are shown in fig 34 and fig 35. The FEA analysis found that the total deformation was 1.76mm located at the rear section of the channel beam. The FEA analysis found that the minimum safety factor was 2.0866 located on the right hand side of the front plate. This indicates that the battery layer 1 can withstand the designated side impact requirement. As discussed previously, an impact on the left hand side is likely to yield similar results.

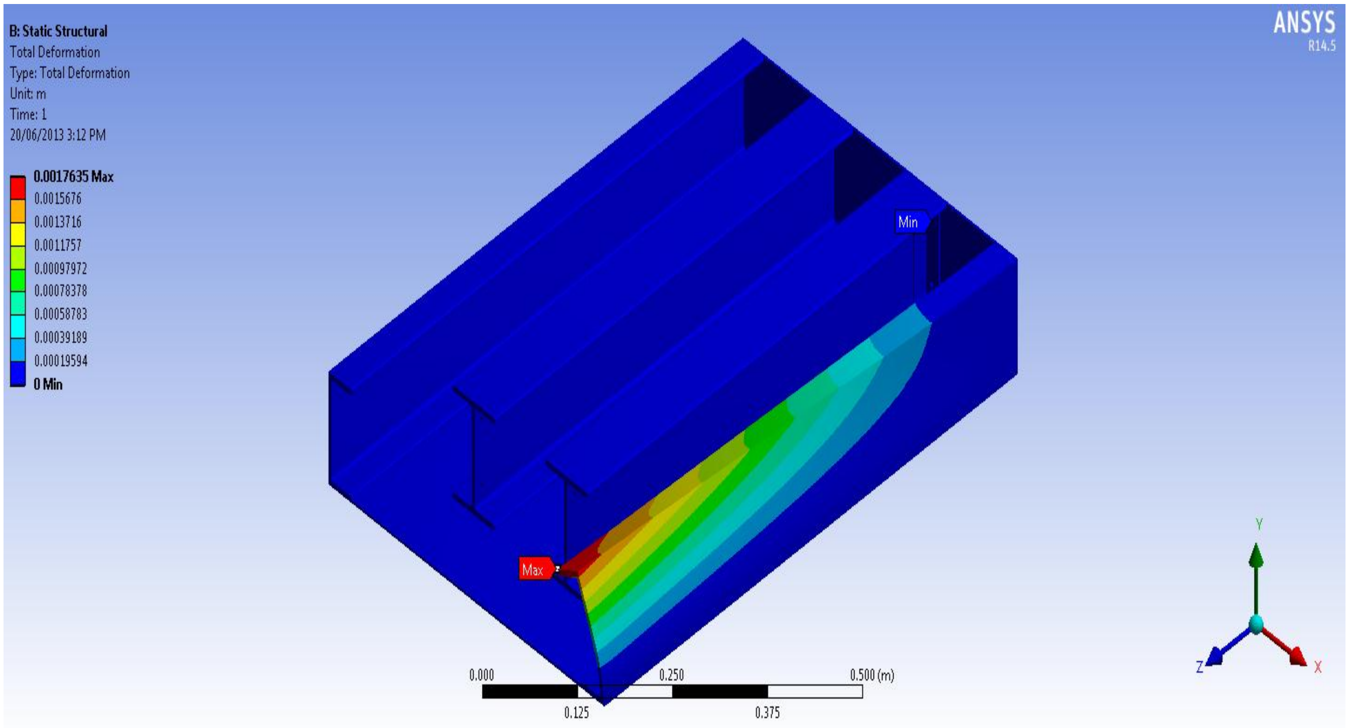

Figure 34 Total deformation side Impact Layer 1

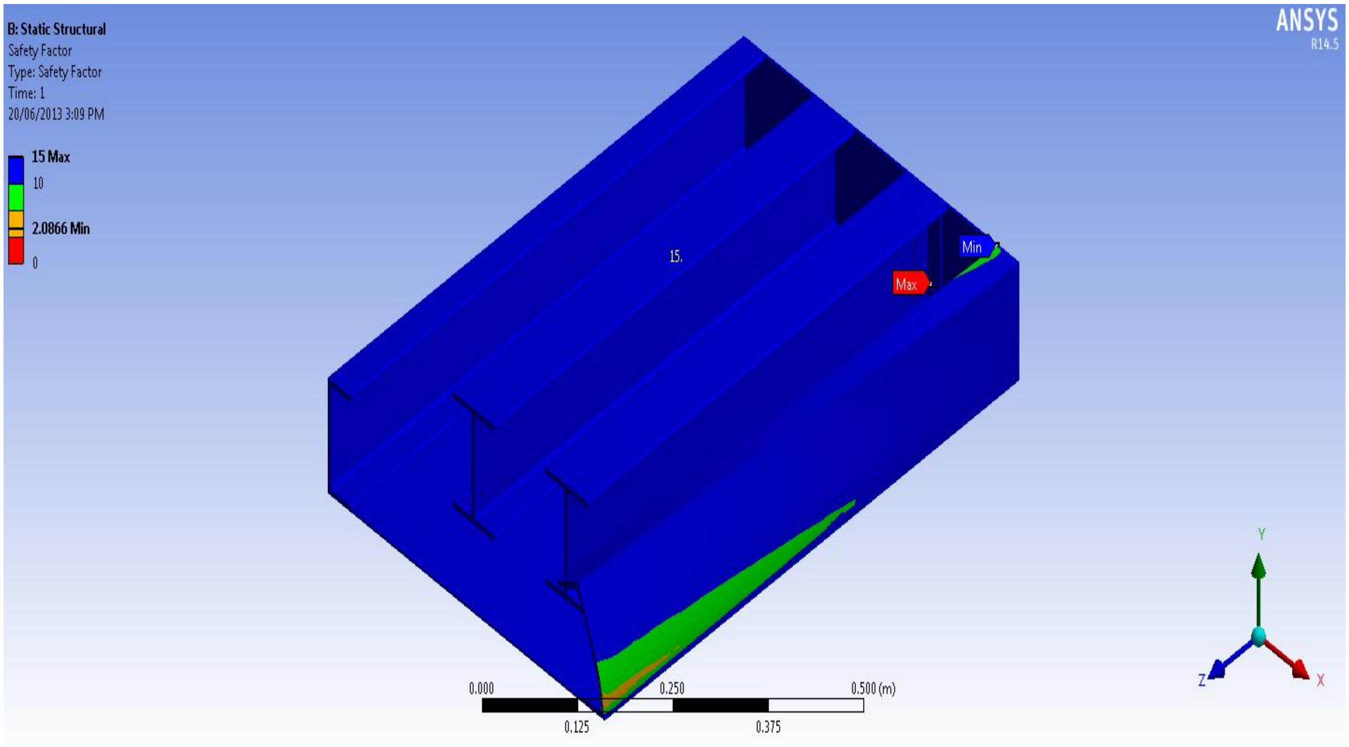

Figure 35 Safety factor, side impact, layer 1

5.3.5.1.3 Vertical Impact

For the vertical impact, the required pressure was applied on 4 faces. The selected are, the top surfaces of the I-beams and the top surfaces of the channel beams. A pressure of 36334Pa was applied on the 4 surfaces. The FEA analysis results for total deformation and safety factor is shown in fig 36 and fig 37. The maximum deformation was found to be 0.301mm, located on the rear section of the channel beams, and the minimum safety factor was found to be 14.19, located on the front plate of layer 1. This result indicates that layer 1 is able to withstand the designated impact acceleration.

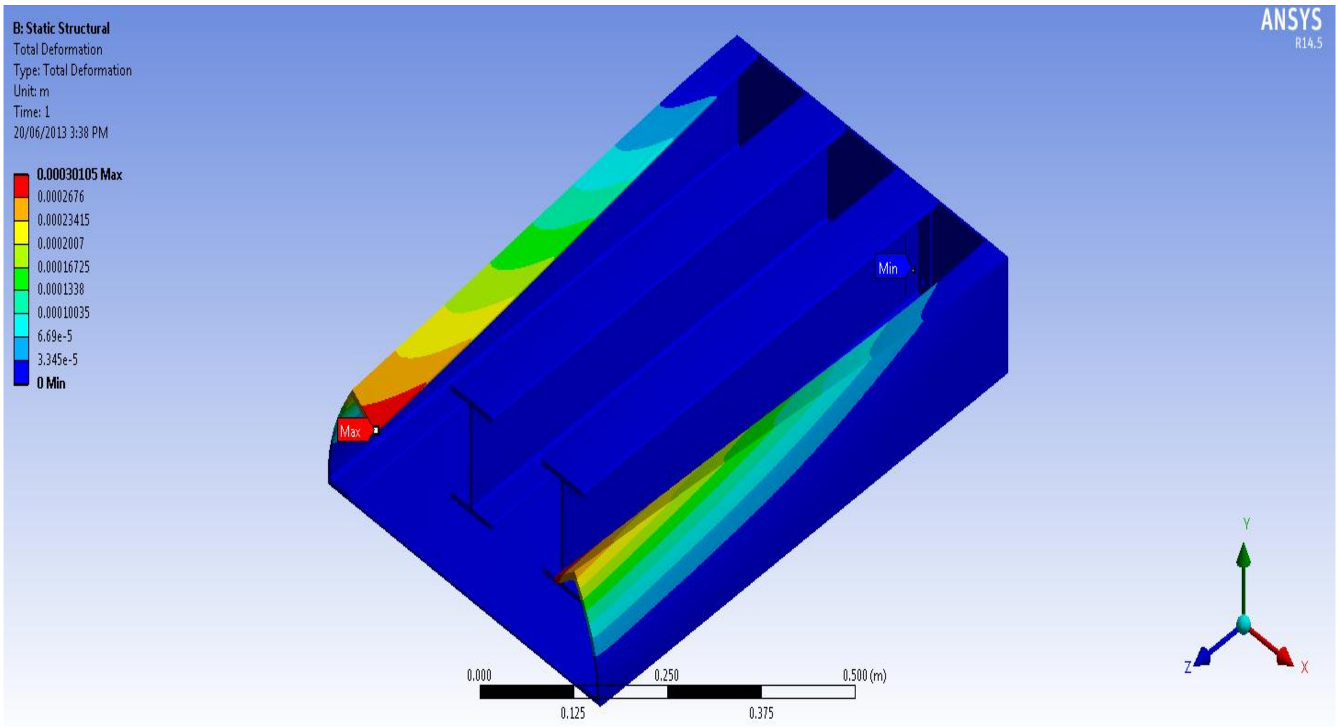

Figure 36 Total deformation, vertical impact, layer 1

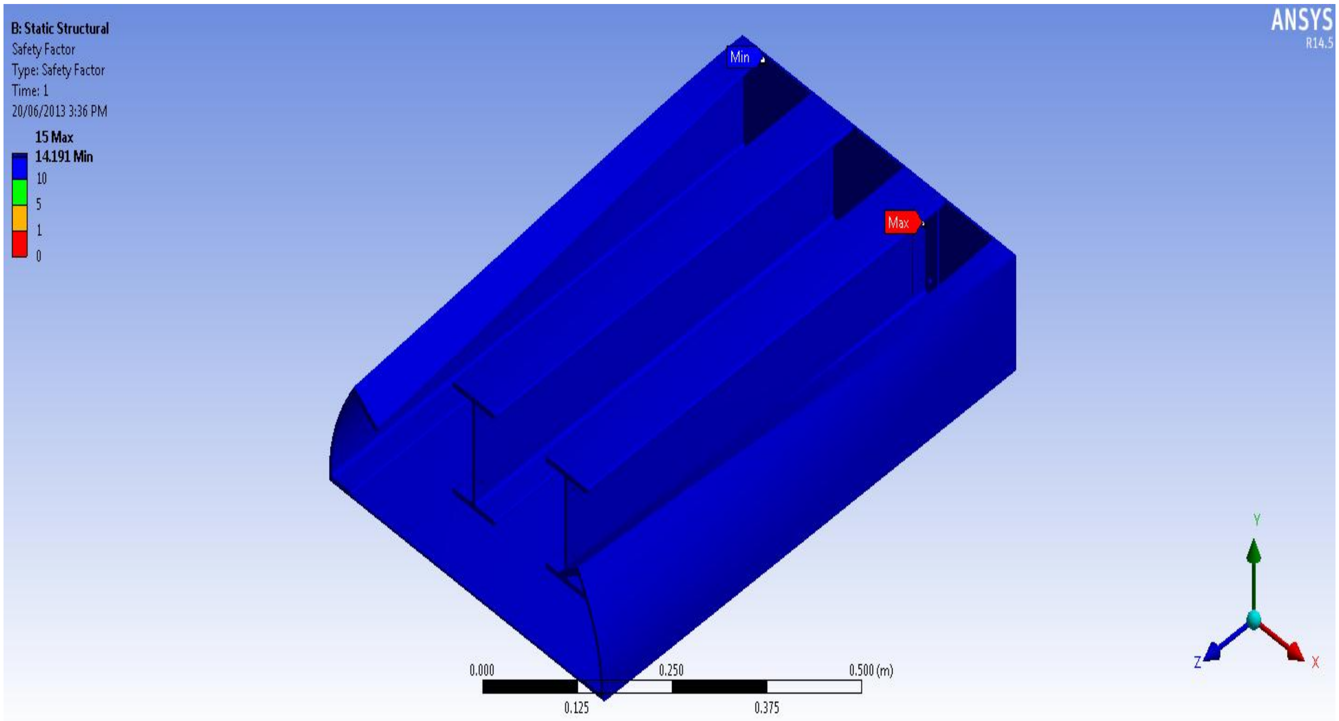

Figure 37 Safety factor, vertical impact, layer1

5.3.5.2 Battery box layer 2

The stress analysis of layer 2 of the battery box is conducted through the use of ANSYS Workbench. Analysis for the front Impact, side impact and vertical impact will be undertaken. The results are shown in the following sections.

5.3.5.2.1 Front Impact

Fig 38 and fig 39 shows the maximum deformation and the minimum safety factor for a front impact on battery box layer 2. The required pressure of 23256Pa was applied to the front section of the battery box layer 2. Through FEM analysis, the maximum deformation was found to be 0.106mm located in the center of the front plate between the two I-beams. The minimum safety factor was found to be 2.8429, located on the edge of the right I-beam. This result indicates that the battery box layer 2 is able to withstand the designated pressure of 23256Pa.

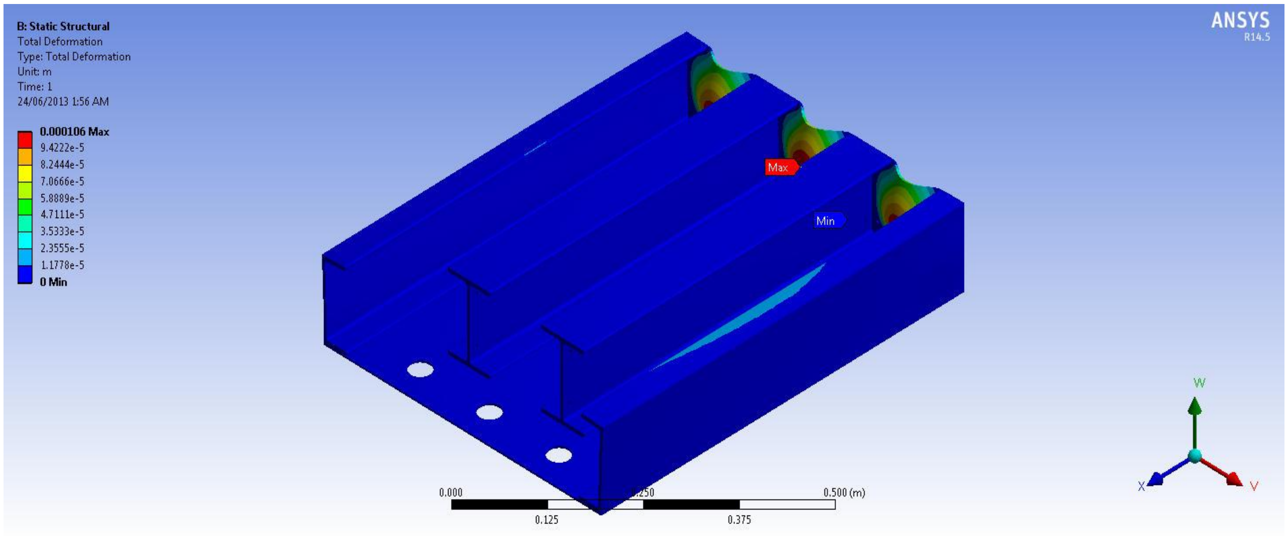

Figure 38 Total deformation, front impact, layer 2

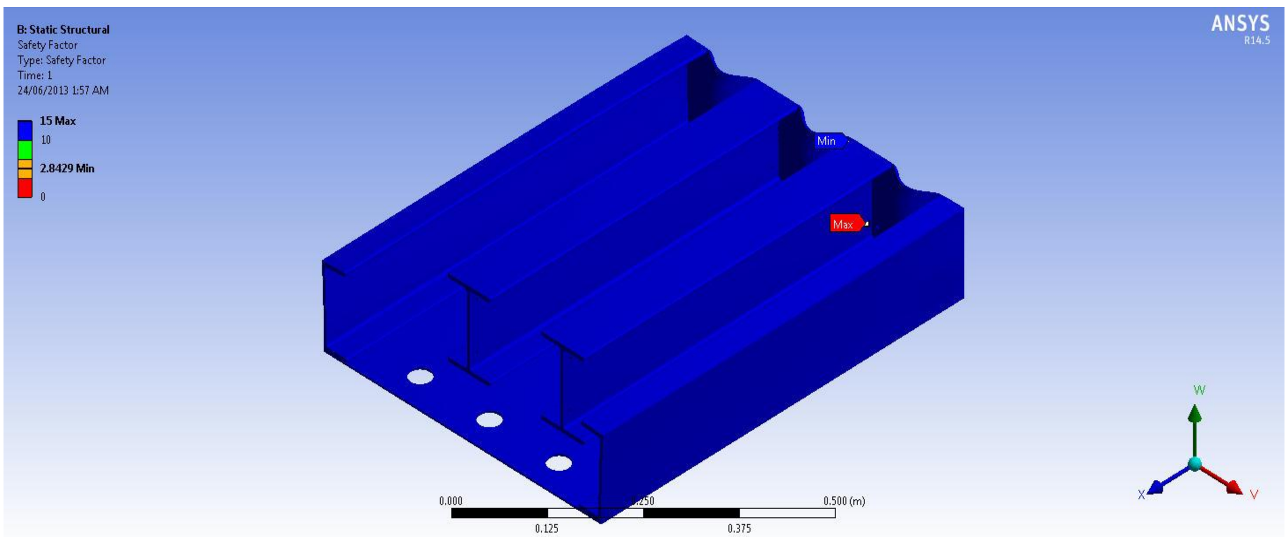

Figure 39 safety factor, front impact, layer 2

5.3.5.2.2 Side Impact

Fig 40 and Fig 41 shows the maximum deflection and minimum safety factor for the side impact scenario. The battery box layer 2 experiences m a much smaller pressure compared to layer 1, however, layer 2 is also slightly smaller in dimensions compared to layer 1. The pressure applied on the side surface is 25484Pa.The FEM analysis found the maximum deformation under the specified pressure to be 1.36mm. The maximum deformation occurs at the rear section of the channel beams.

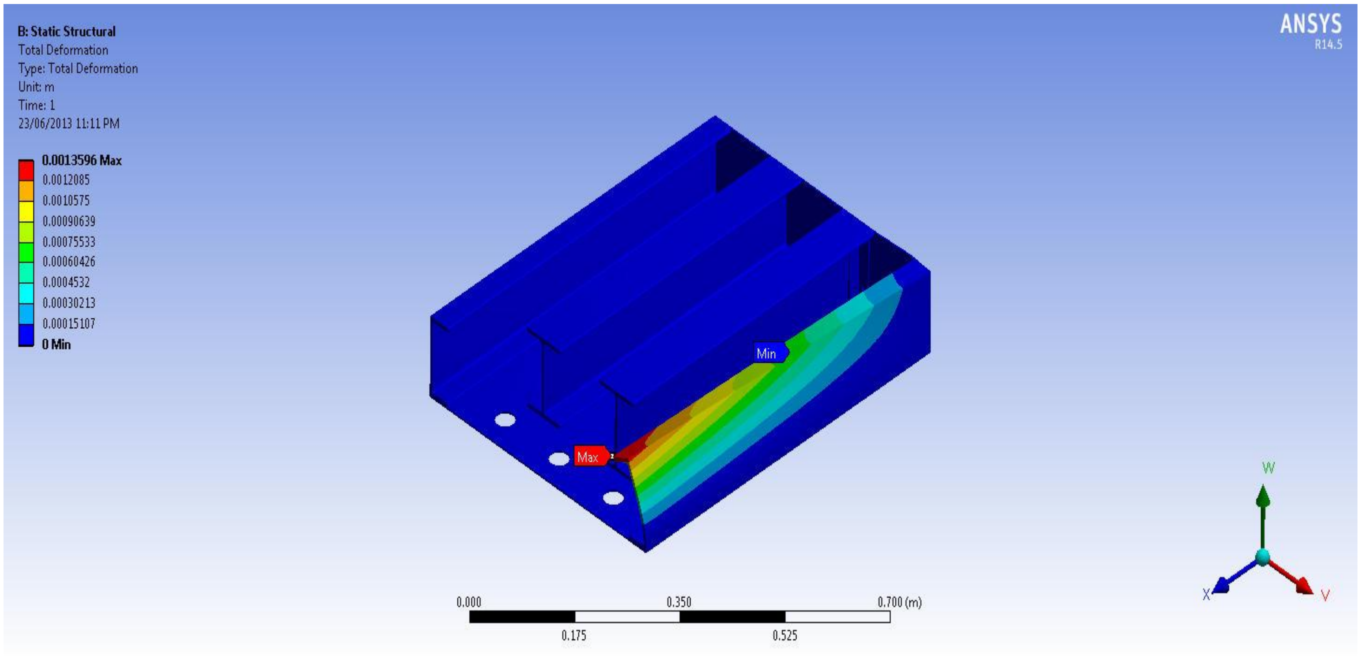

Figure 40 Total deformation, side impact, layer 2

The FEM analysis found the minimum safety factor to be 3.326. The minimum safety factor was located on the right hand side of the front plate where the plate makes contact with the channel beam. This result indicates that the battery box layer 2 is able to withstand the specified pressure 24235Pa. An analysis for the right hand side impact scenario was not undertaken as the structure is designed to be symmetric along the centerline. Thus an impact on the right hand side would also yield similar results (see section 5.3.5.1.2 for more details).

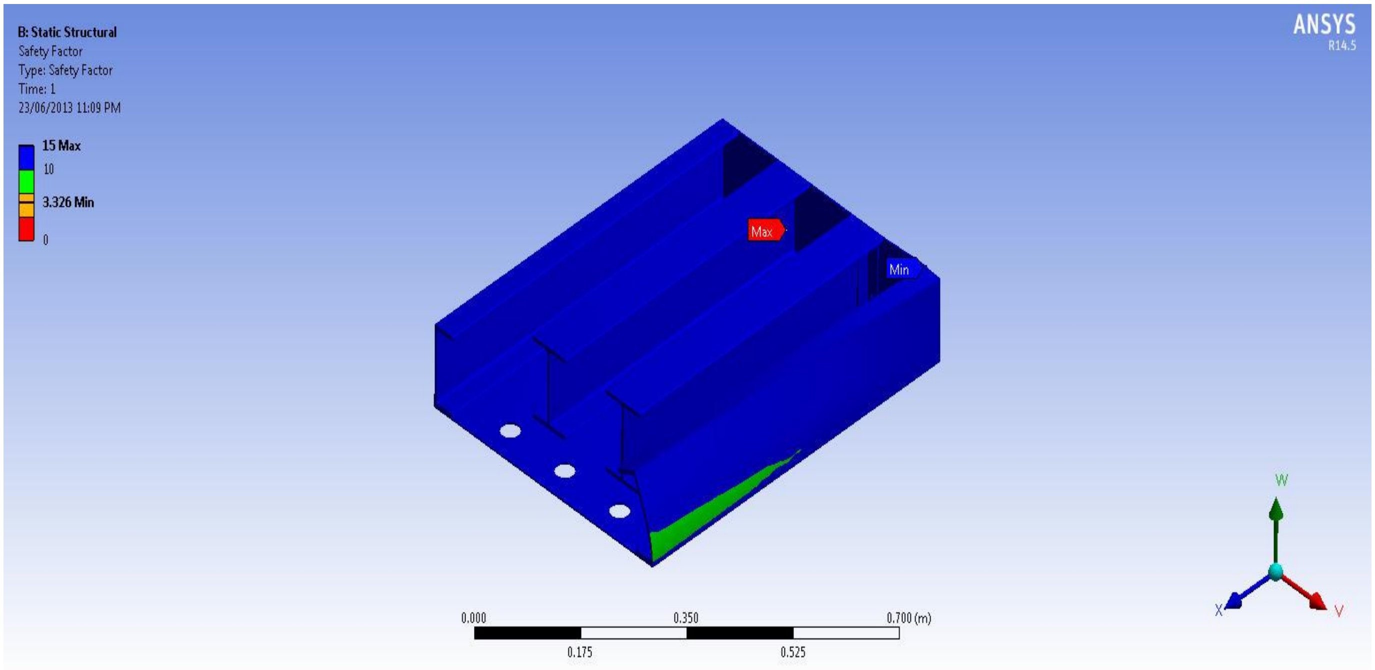

Figure 41 Safety factor, side impact, layer 2

5.3.5.2.3 Vertical Impact

Fig 42 and Fig 43 shows the maximum deformation and minimum safety factor for a vertical impact. The pressure applied in this scenario is 24235Pa. The pressure was applied on 4 surfaces, Top surfaces of the I-beams and the top surface of the channel beams. As it can be seen from fig 42, FEM analysis has revealed the maximum deformation to be 0.23mm. The maximum deformation is located on the towards the rear section of the left channel beam. The minimum safety factor was found to be 14.087 located on the left I beam. This indicates that the battery box layer 2 is able withstand the specified pressure of 24235Pa adequately.

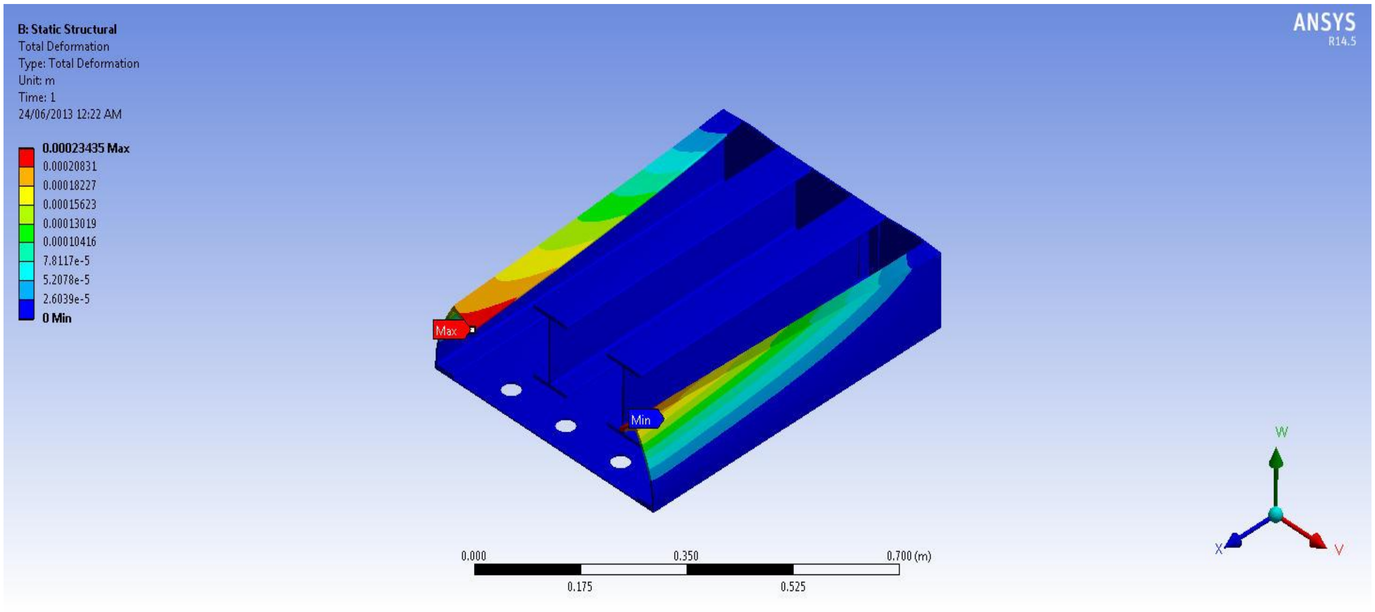

Figure 42 Total deformation, vertical impact, and layer 2

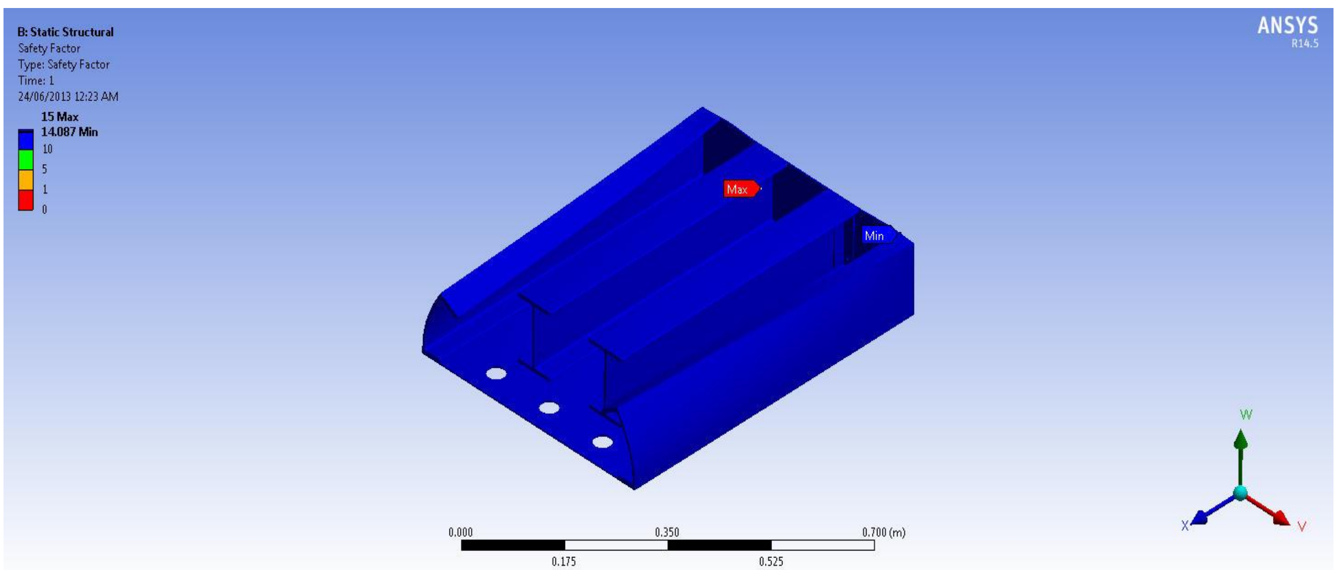

Figure 43 Safety factor, vertical impact, and layer 2

5.3.5.3 Battery box layer 3

The dimensions for the battery box layer 3 are identical to that of the battery box layer 2. As it can be seen from table 5, the required pressures for battery box layer 3 are smaller than the required pressure for battery box layer2. Since both layer 2 and layer 3 is constructed using Aluminum alloy, layer 3 and layer 2 also possess identical material properties. Thus it can be concluded that if the minimum safety factors for layer 2 are above 1 for all scenarios, then the layer 3 can be assumed have a minimum safety factors of above 1 for all scenarios as well.

5.3.6 Summary

In conclusion the finite element analysis was successfully utilized to investigate the reliability of the final design of the battery restraining system. The results obtained from the FEA testify that the current battery restraining system design can withstand the impact requirements outlined in section 4.4.2. This conclusion was reached due to the minimum safety factor values have exceeded 1 in all impact scenarios.

5.3.7 Limitation of Finite element Analysis

Finite element analysis applied on the battery box assumes that all impact pressure is distributed evenly on one surface of the battery box layer. This is an unrealistic assumption as an impact on the battery restraining system is likely to be a sudden force applied to one point of the battery box.

The accuracy of the FEA model greatly depends on the material properties of the battery restraining system. If the material properties of the battery restraining system changed due to thermal expansion the reliability of the FEA analysis cannot be guaranteed (Logan, D 2012).

5.3.8 Fabrication

Upon completing the FEA analysis the final design was approved for construction. I-beams were purchased from One Steel Aluminum located in Bibra lake. The I-beams were subsequently submitted to the physics workshop to be cut into appropriate lengths (668mm and 568mm beams). The remaining I-beams were used to construct Channel beams for the side supports of the battery box. The channel beams were constructed by sawing one side of the I-beam flange. The Channel beams were subsequently cut into appropriate lengths (768mm and 668mm).

Aluminum alloy sheets were used to create the lid and the base plate of the battery box. These items were fabricated through G&C Sheet metal, also located in Bibra lake. Polycarbonate sheets for insulations purposes were cut and installed in to battery box through the physics workshop. Finally, plastic hold downs were purchased from Clark rubber to restrain the battery modules.

3M VBH double sided adhesive tapes have been purchased from the 3M website. Upon arrival, the assembly process can commence.

6 Design of the motor mounting system

6.1 Overview

The REV Jet Ski's propulsion system was intended to be an AC induction motor which can produce 50kW of power and has a voltage rating of 96V. The electric motor must be small enough to be able to lower into the Jet Ski through the opening under the Jet Ski seat. The motor was intended to be placed in the aft section of the Jet Ski where the petrol motor of the original Jet Ski was also placed. As the shaft connected to the propeller of the Jet Ski is located in the aft section of the Jet Ski, the aft section was the logical place to install the electric motor. The electric motor will be mounted to the Jet Ski using mounting points 3, 4, and 5 (see fig 4) located in the aft section of the Jet Ski. In this particular chapter, the design of the motor mounting system will be discussed in detail.

6.2 Design Methodology

6.2.1 Design requirement for the motor mounting system

The design requirement of the motor mounting system is listed below.

1. The motor mounting system must restrain the motor in all directions such that the motor will be held in place during an impact.
2. The motor must be mounted in a manner which allows easy access to the electrical components mounted on the motor. This will improve serviceability of the motor as well as the electrical components.
3. The mounting system must withstand the peak operating impact g-forces outlined in the section 4.5.
4. Existing mounting points must be used for the mounting of the electric motor to mimic the weight distribution of the original Jet Ski.

6.2.2 Design process

The design process of the motor mounting system is outlined below.

1. Create design concepts for the motor mounting system and discuss the design with the supervisor and the REV Jet Ski team members. The concept designs must address the constraints imposed on the creation of the motor mounting system.
2. Create a computerized 3D model of the motor mounting system and submit the designs to the relevant workshop for a cost estimate for fabrication.

3. If the quoted cost is reasonable, submit a final SolidWorks design to the relevant workshop for fabrication. If the cost was deemed too expensive, advice must be sought from the workshop to identify aspects of the design that could be modified to lower the cost of fabrication.
4. If the material used for the fabrication of the motor mounting system is light weight and low strength material, a stress analysis through ANSYS workbench is performed to ensure that the mounting system would not fail under peak performance loading from the Jet Ski.

6.3 Initial design and final design

6.3.1 Initial design

The initial design for the motor mounting system was designed with consideration for the design requirement shown in section 6.2.1. However in the early stages of the project, REV Jet Ski team members were still investigating numerous types of motors which could satisfy the requirement of producing 50kW of power while having a voltage rating under 100V. Thus, an initial design was proposed which could accommodate various dimensions. The initial design is shown in fig 44

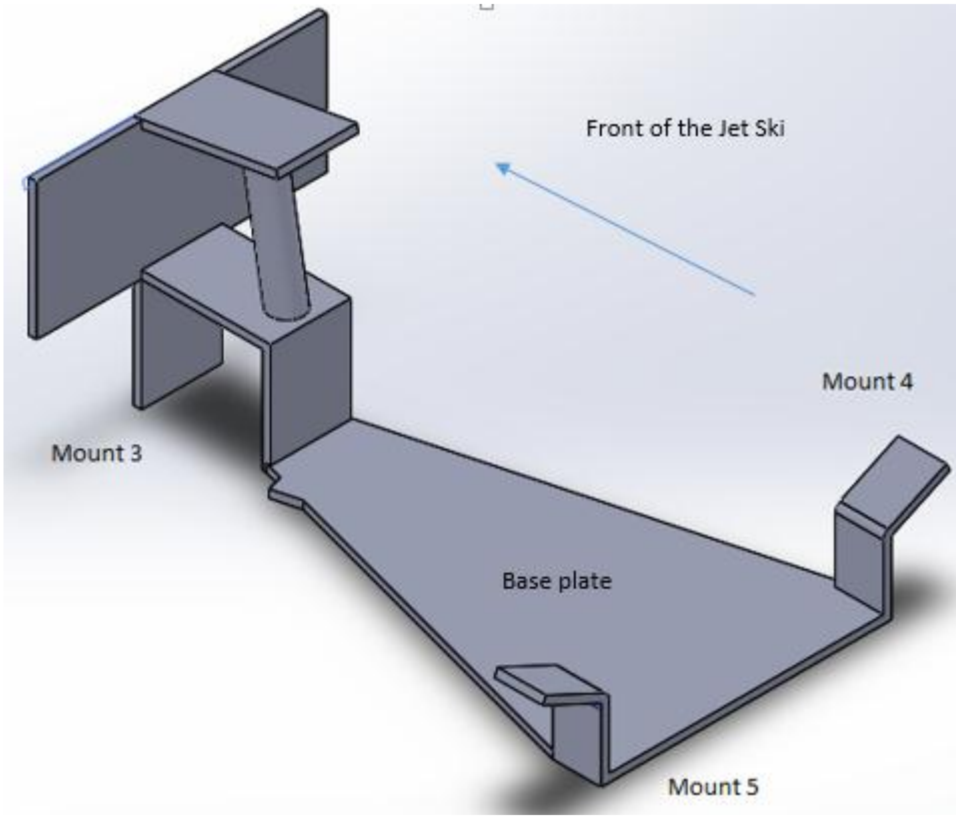

Figure 44 Initial design for the motor mounting system

The motor was intended to be mounted on the base plate as shown in fig 44. The design would require the base plate to be cut from a single sheet of Aluminum alloy, and features such as mount 3, mount 4 and mount 5 shown in fig 45 would be fabricated through a workshop and welded on to the base plate. This design was accepted as an initial concept design, however it presented a limitation that caused the design to become unviable.

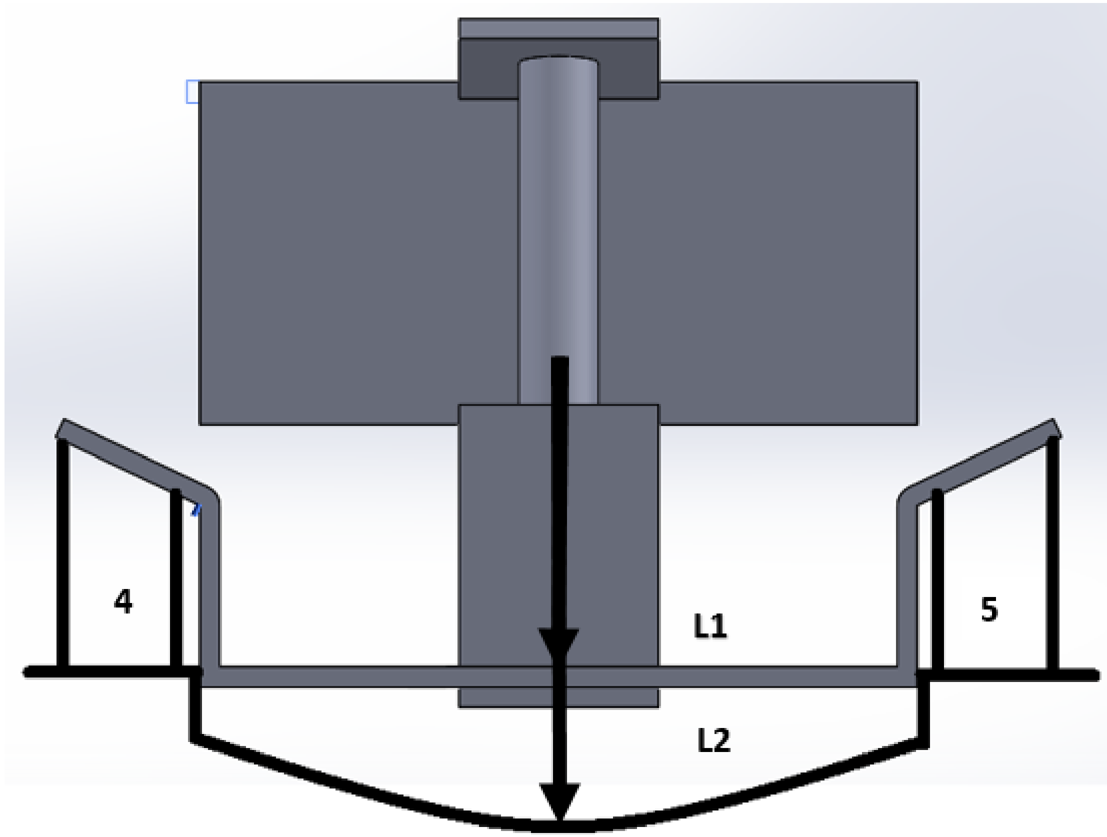

Figure 45 Aft view

The limitation of the initial concept design is further illustrated in fig 45. Fig 45 is the rear view of the concept design, mounting points 4 and 5 are also shown in this drawing to demonstrate how the mounting system will be placed. The contours of the inside of the Jet Ski hull is outlined as seen from figure 45. This figure illustrate that there is a region above the base of the hull indicated by $L2 - L1$ ($L1$ and $L2$ are measured from the position of the shaft) that cannot be used due to the base plate of the motor mounting system. Thus this motor mounting system severely limits the possible dimensions of the motor that could be used. Due to this limiting factor this concept design was not pursued further.

6.3.2 Final design and discussion

The final design of the motor mounting system was created through collaboration with Submersible Motors Engineering (SME). SME has extensive experience in designing water proof AC induction motors for the oil and gas industry. The REV Jet Ski team was unable to find a suitable AC induction motor which full filled the requirement of a power rating of 50kW as well as a voltage rating of 96V. Thus Submersible motors were contacted to build a custom motor for the REV Jet Ski. SME generously provided assistance developing an AC induction motor and agreed to donate the motor to the REV Jet Ski program. During the Development phase the limiting factors for the previous motor mounting system was discussed with SME engineers. Through collaboration with SME engineers the final design of the motor mounting system was produced, the final design is shown in fig 46. To ensure that the most of the available space within the aft section is used, the mounting brackets for the SME induction motor was welded on to the motor directly.

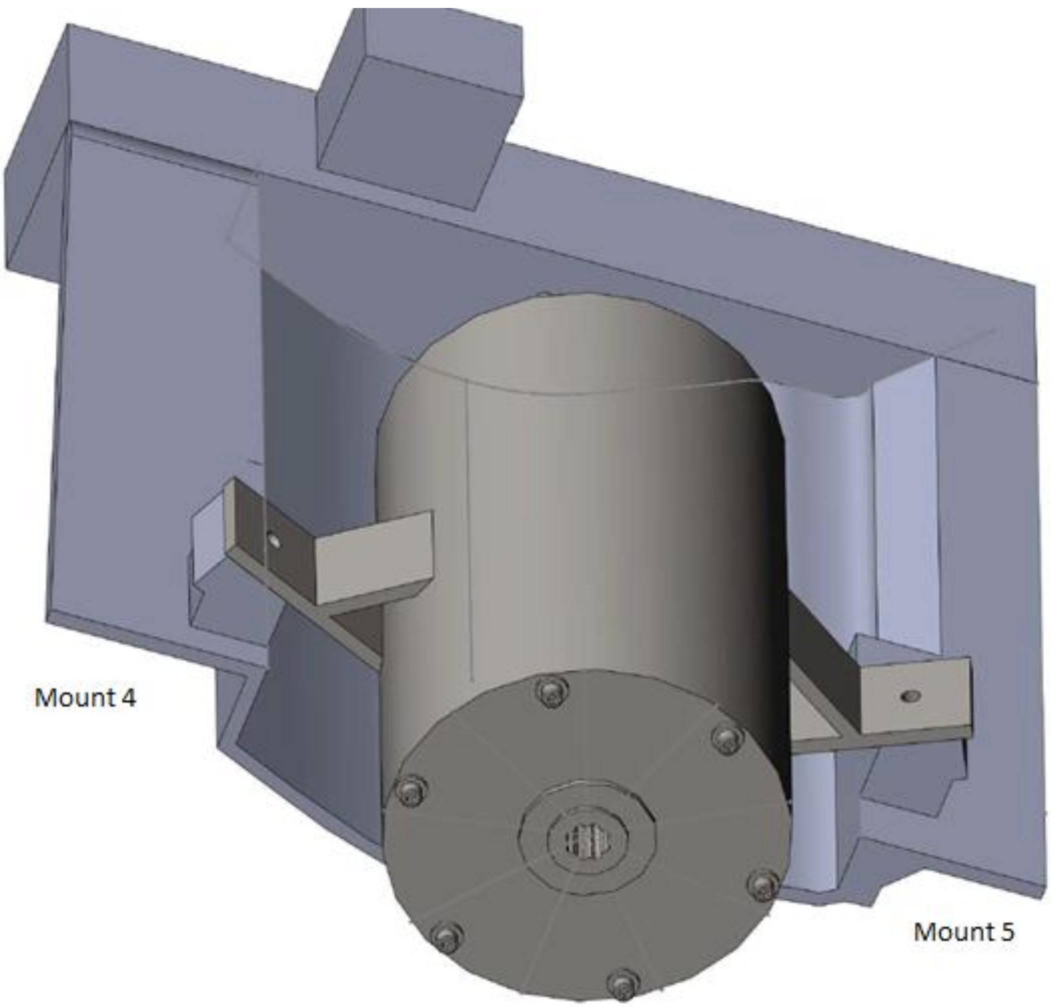

Figure 46 Final design

As seen from fig (), a mounting bracket that could be welded directly to the motor was designed. A third mounting bracket was also designed which could mount the motor on to mounting point

3, The detailed drawing of the mounting brackets and the motor is shown in Appendix E. This drawing was supplied to the REV Jet Ski team through SME. The SME engineering team is currently performing a stress analysis on the motor mounting bracket using Aluminum alloy and stainless steel as a possible material to be used. The stress analysis will be conducted using the impact requirement outlined in section 4.5. Once the stress analysis is complete, the material will be chosen to fabricate the motor mounting bracket. SME has also agreed to install the motor and the motor mounting system in their warehouse located in Maddington.

7 Conclusion and future works

The battery restraining system for the REV Jet Ski is nearing completion as per the requirements set by the NCOP and ADR as well as the impact data obtained through the experiment (see 4.4.2). An in depth stress analysis was carried out using Solid Works and ANSYS workbench to obtain the ideal design. The battery restraining system was able to be designed in a manner which did not affect the weight distribution of the Jet Ski. The I-beams, Channel beams and the Aluminum sheet metals used for the fabrication and assembly have been purchased. The assembly of the battery restraining system can now commence. However, a rear stopper for the battery box still needs to be designed and fabricated.

The final design of the motor mounting system has been completed through extensive collaboration with the SME engineers. A stress analysis is currently being performed at SME the experiment data obtained (see section 4.4.2). Upon completion of the stress analysis, fabrication of the motor mounting system will be carried out.

Upon future completion of the REV Jet Ski, The REV Jet Ski team will be required to license the electric Jet Ski to allow normal operations within the Swan river area. The marine safety officer will also be contacted to inspect the Jet Ski and

8 References

Australian Motor Vehicle Certification Board Working Party 2006, *NCOP14 Guidelines Electric Drive*, Australian Motor Vehicle Certification Board Working Party, Australia

Brant, B 1994, *Build Your Own Electric Vehicle*, TAB Books, United States.

Brown, MP 1993, *Convert It*, Future Books, United States.

Degarmo EP, Black JT & Kohser RA 2003, *Materials and processes in manufacturing*, Wiley, United States

Dotmar 2012, *Safeguard PC Premium Quality Polycarbonate*, DEP Products, Dotmar Engineering Plastic Products.

ECOwatercraft, *ECOwatercraft*, ECOwatercraft. Available from: <http://www.ecowatercraft.com/>. [9 October 2012].

Gulf Coast Data Concepts 2007, *GCDC X16-1C User Manual*, Gulf Coast Data Concepts. Available from: http://www.gcdataconcepts.com/GCDC_X16-1C_User_Manual.pdf [16 February 2013]

Headway Headquarters, *38120S*, Headway Headquarters. Available from: <http://headway-headquarters.com/38120s/>.

Hooper, I. 2011. *Development if In-Wheel Motor Systems for Formula SAE Electric Vehicle*. BEng. Thesis. University of Western Australia: Australia

Jones, D 1996, *Principles and prevention of Corrosion,* 2^{nd} edn, Prentice Hall, United States

Logan, D 2012,*A First Course in the Finite Element Method,*5^{th} edn, Cengage Learning, United States

Mathew R 2008, *Welcome to the REV Project*, REV Project, University of Western Australia, Available from: <http://www.therevproject.com/> [14 September 2012]

Mathys, C 2004, *Electric Propulsion for Boats*, Netcam Publishing, Naples Florida

OneSteel 2013, *OneSteel Aluminium National Catalogue*.

Pachauri, RK & Reisinger, A 2007, Climate Change 2007 Synthesis Report, Intergovernmental Panel for Climate Change, [April 2013]

Standards Australia 1996*, AS/NZS 1866:1997: Aluminum and aluminum alloy – Extruded rod, bar, solid and hollow shapes*, SAI Global.

Standards Australia 1998, AS 4100-1998*: Steel structures*, SAI Global, Strathfield NSW.

Standards Australia 2009, AS 1799.1: 2009 :*Small crafts,* SAI Global, Strathfield

Sea-Doo 2007a, *2008 Operator's Guide*, Bombardier Recreational Products.

Sea-Doo 2007b, *2008 Shop Manual*, Bombardier Recreational Products.

SME, *Company Profile*, Submersible Motor Engineering. Available from: http://smeng.com.au/ [April 2013]

Tan, D. 2008. *Design and Construction of Motor Mounts for the Renewable Energy Vehicle*. BEng. Thesis. University of Western Australia : Australia

ThunderSky 2007, ThunderSky, *Lithium Ion Power Battery Specification,* ThunderSky. Available from: http://liionbms.com/pdf/thundersky/TS-LFP100.pdf [December 2012]

UWA Occupational Therapist, *Safety in Workplace*, UWA. Available from : http://www.safety.uwa.edu.au/policies/safety_in_workshops[March 2013]

UWA Safety & Health Manager 2007, *UWA Electrical Safety Pamphlet*, UWA, Perth

Appendix A Card Board Profiles

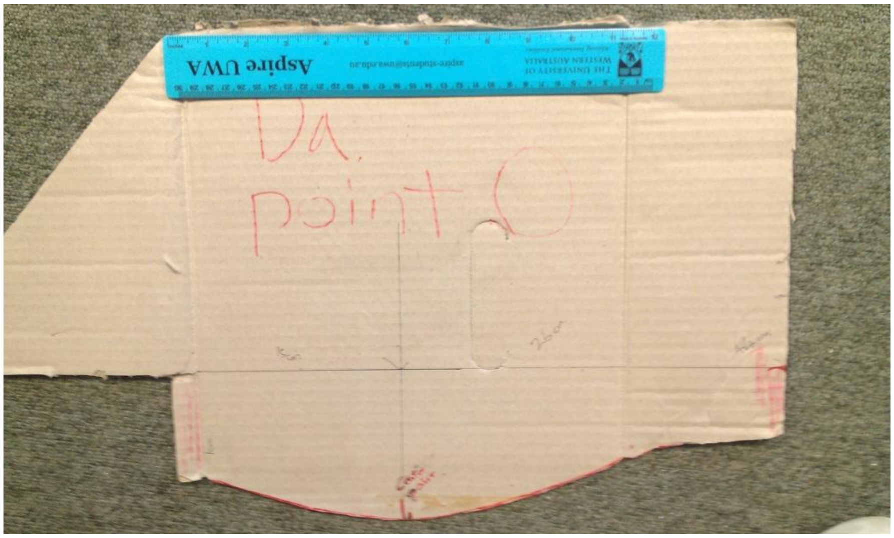

Figure 47 Profile 1 Origin

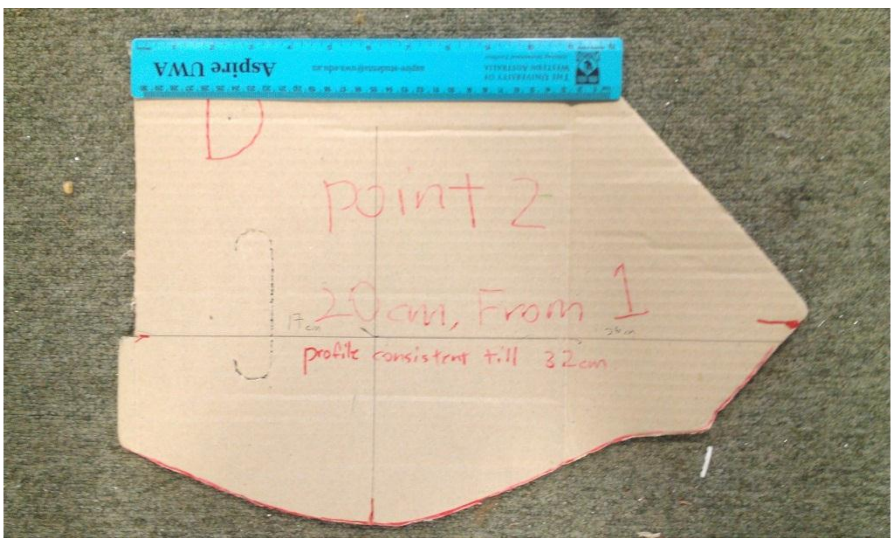

Figure 48 Profile 2

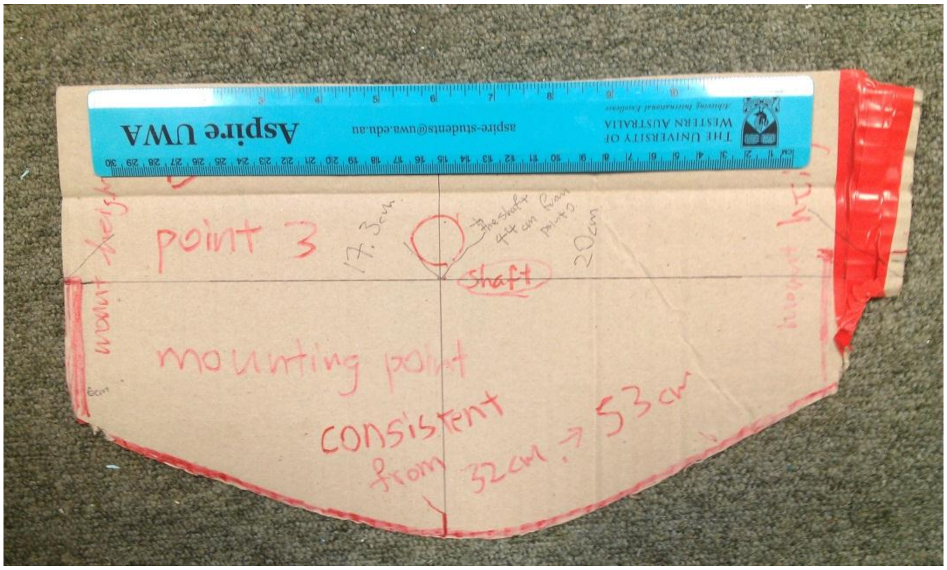

Figure 49 Profile 3

Appendix B

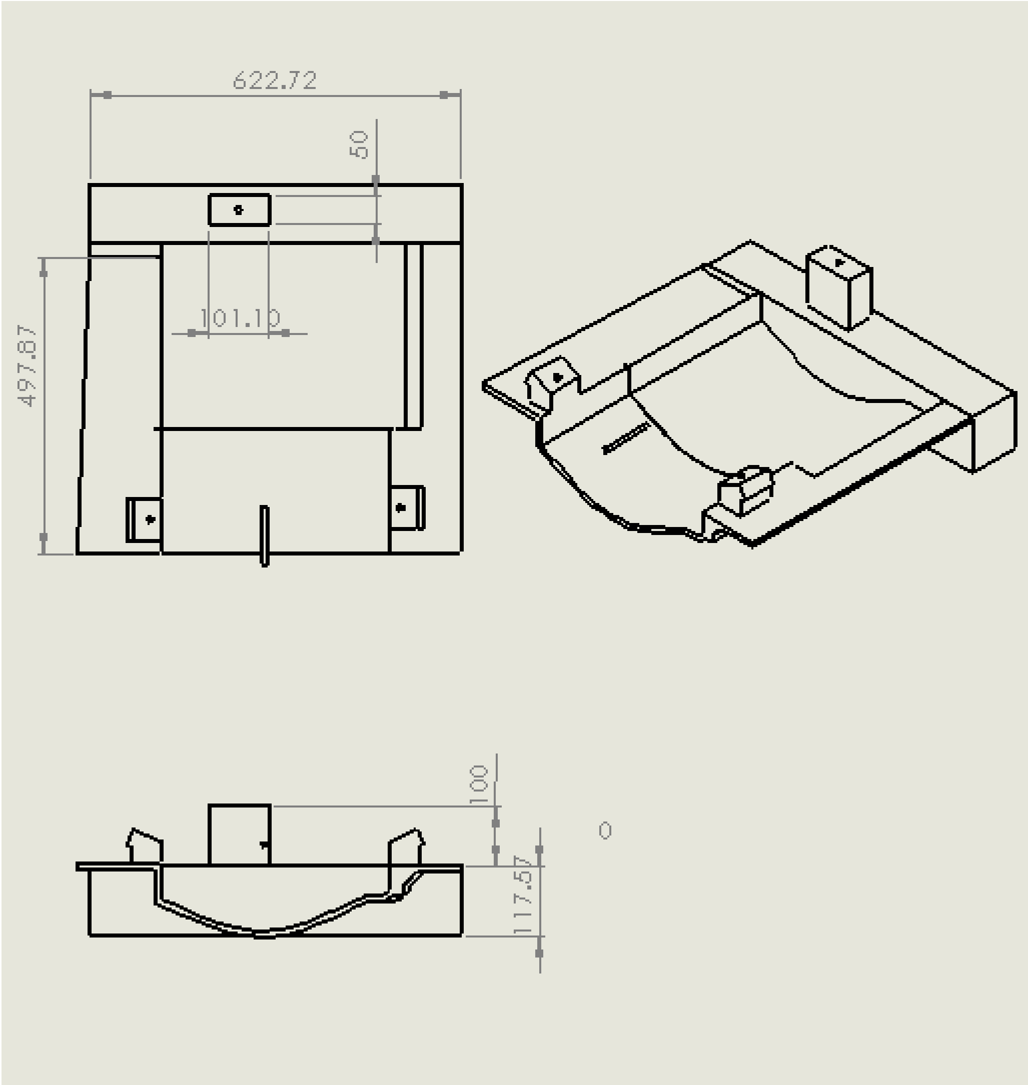

Figure 50 Dimensions for the surface map.

Appendix C

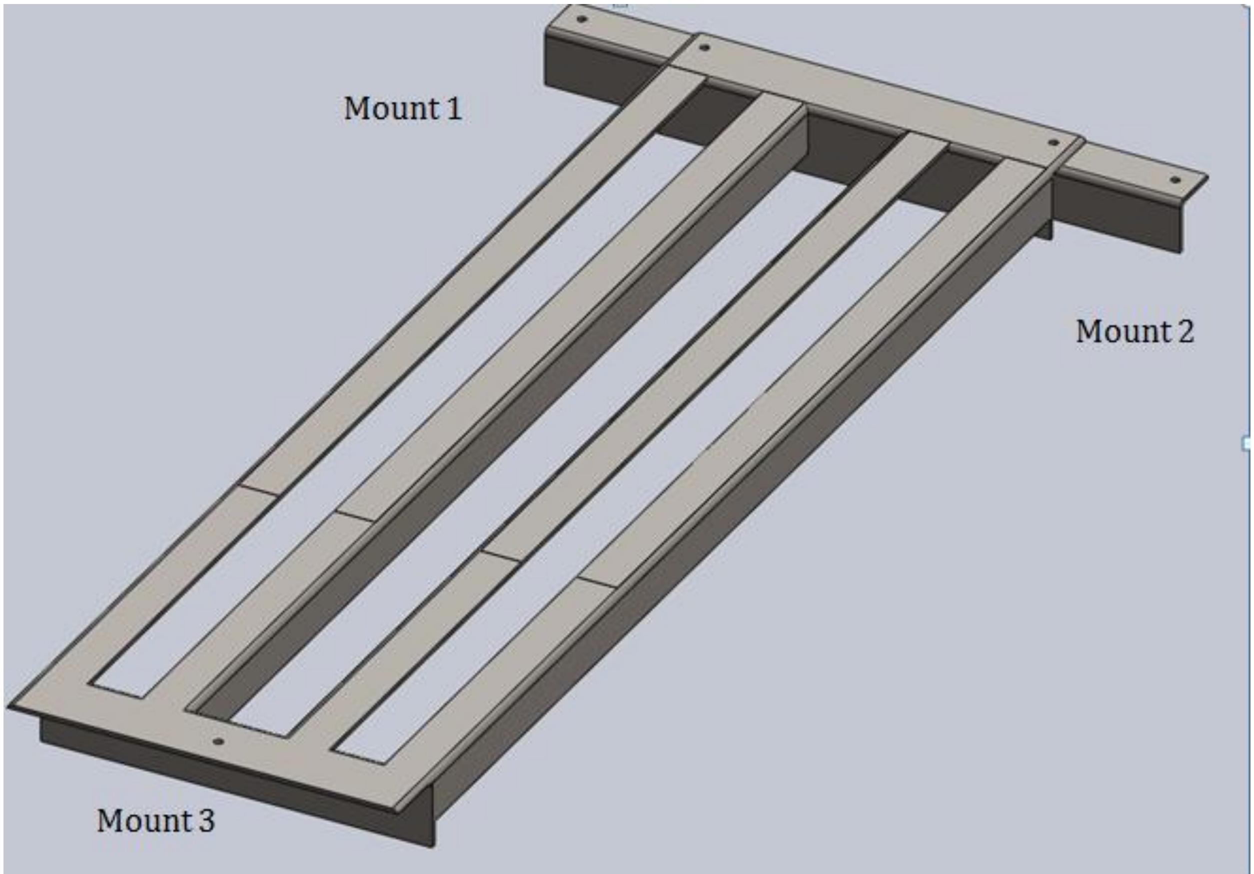

Figure 51 Support Frame design

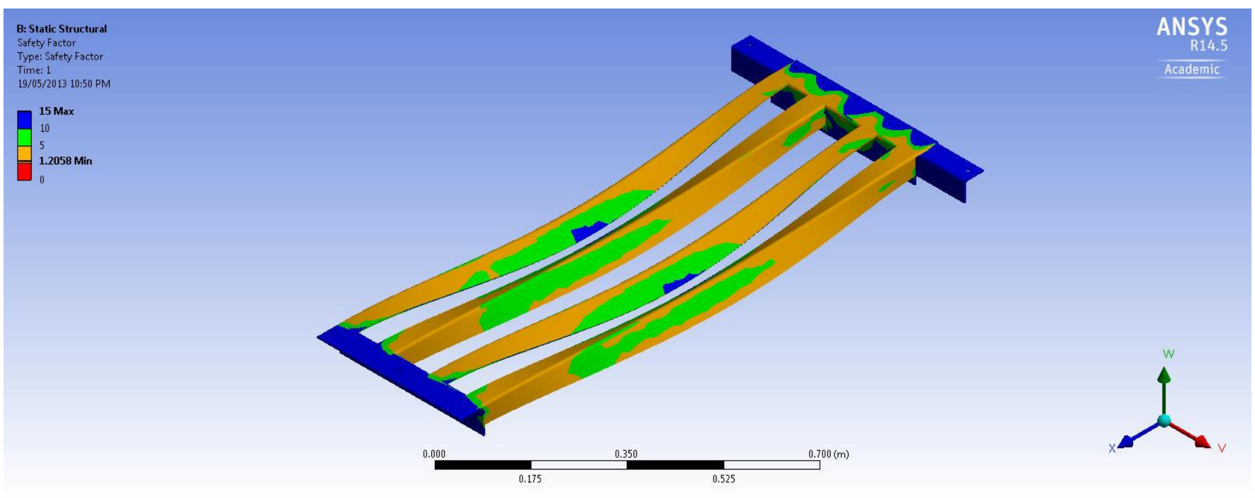

Figure 52 Support mount Vertical Impact of 10g

The support mount was able to achieve the safety factor of 1.2 at 10g acceleration of the battery box structure. This indicates the Structure is can withstand the pressure applied.

Appendix D

The detailed drawing of the motor mounting system is shown below. Figure 53,and figure 54 are provided by Submersible Motors Engineering.

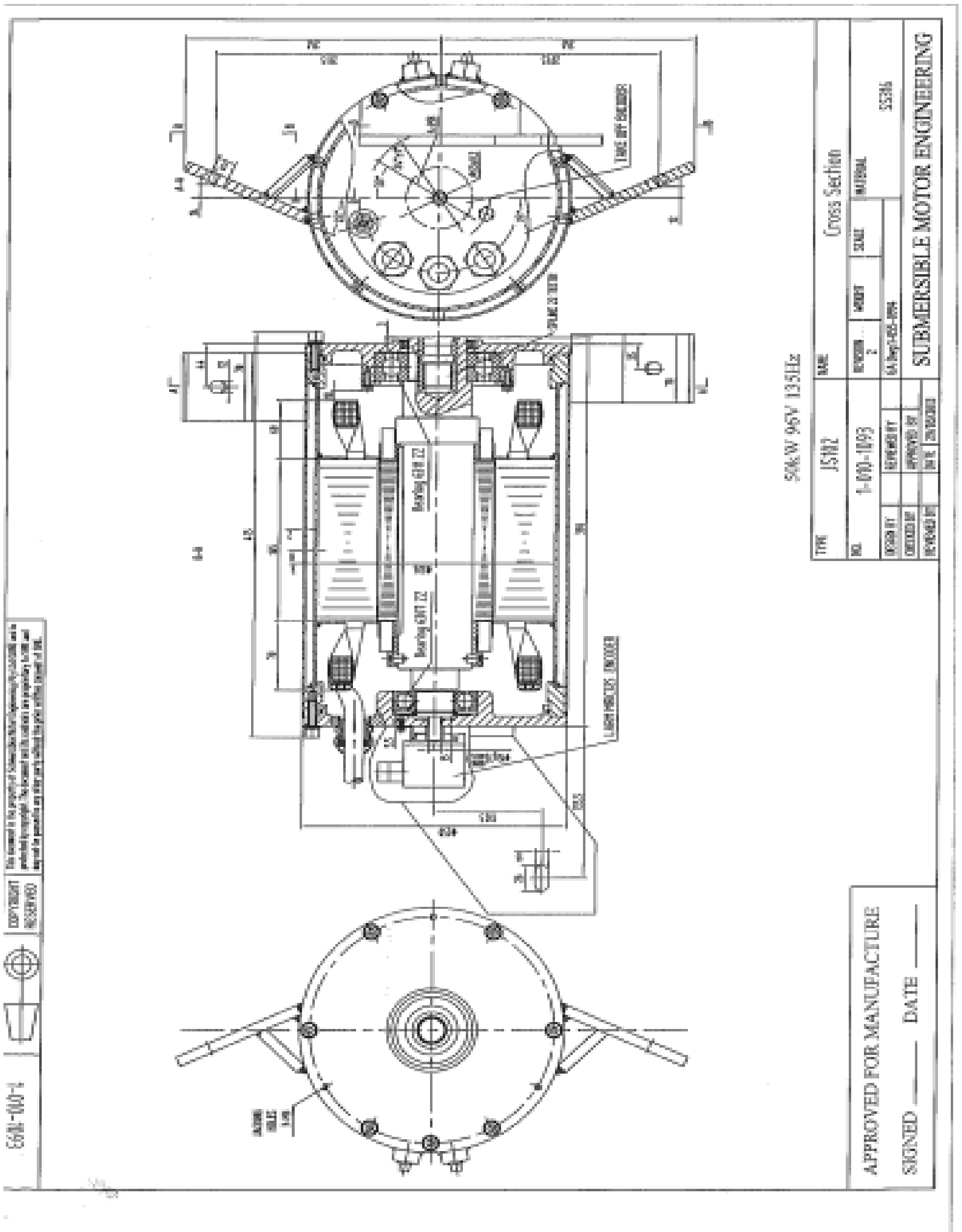

Figure 53 Motor mounting system and the motor

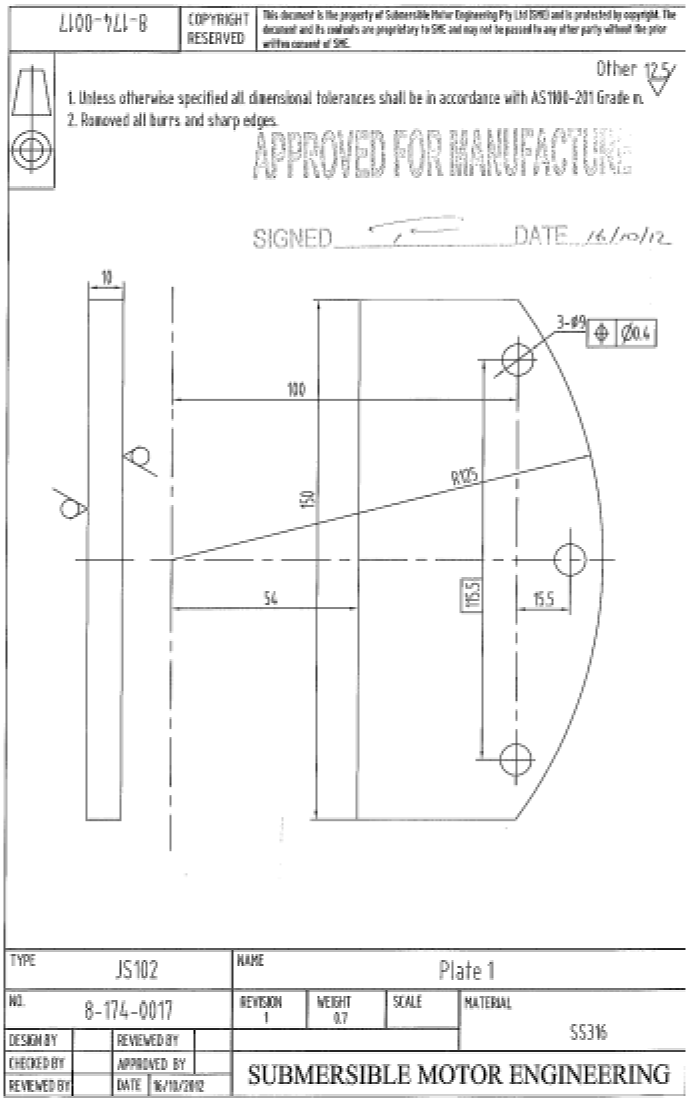

Figure 54 Bracket Design for mounting point 3

Appendix E

Data sheet for 3M double sided adhesive tapes are shown below.

3M™ VHB™ Tape Families:

4941 This family utilizes multi-purpose acrylic adhesive on both sides of conformable foam. The adhesive pr[illegible] excellent adhesion to a broad range of high and medium surface energy substrates including metals, glass, and a wide variety of plastics, as well as plasticized vinyl. The conformable foam provides good contact, even with mismatched substrates. Available in gray and black.

5952 This family matches the modified acrylic adhesive on both sides of very conformable foam, providing adhesion to the broadest range of substrates, including most powder coated paints. Available in black.

4950 This family has general purpose adhesive on both sides of firm type foam. This family is typically used on metal, glass and high surface energy plastic substrates. Available in white and black.

4945 This family has multi-purpose adhesive on both sides of firm foam. Available in white.

4910 This family of clear tapes is excellent for applications where clear or colorless is desired. The general purpose adhesive on both sides is suitable for high surface energy substrates.

4951 This family of tapes is based around the low temperature appliable acrylic adhesive system, utilized on both firm and conformable foam types. These products are suitable for high surface energy substrates. Available in white (firm foam) and gray (conformable foam).

4952 This family utilizes the low surface energy adhesive on a firm foam. Available in white.

4611 This family has a general purpose adhesive on both sides of firm foam. This family of tapes is typically used on metal substrates, and has the added feature of high temperature resistance, making it often suitable for bonding prior to high temperature paint processing. Available in dark gray.

4622 This family has general purpose adhesive on the face side (the side that typically would be bonded first) and multi-purpose adhesive on the liner side (the side exposed when the release liner is removed) of a conformable foam. Available in white.

3M™ VHB™ Tape Product Family Guide

Thickness inches (mm)												
Family ▶	4941		5952	4950		4945	4910	4951		4952	4611	4622
Color ▶	Gray	Black	Black	White	Black	White	Clear	White	Gray	White	Dk Gray	White
Foam type ▶	Conform	Conform	Very Conf	Firm	Firm	Firm	n/a	Firm	Conform	Firm	Firm	Conform
Adhesive ▶	Multi-Purpose		Modified	General Purpose		Multi-Purp	Gen-Purp	Low Temp Apply		LSE	Gen-Purp	Gen/Multi
0.010 (0.25)				4914								
0.015 / 0.016 (0.4)	4926		5915 5915P	4920								
0.020 (0.5)							4905					
0.025 (0.64)	4936 4936F	4919F	5925 5925P	4930 4930F	4929					4932	4646	4618
0.032 (0.8)			5930 5930P									
0.040 (1.0)			5958FR				4910					
0.045 (1.1)	4941 4941F	4947F	5952 5952P	4950	4949	4945 4946		4951	4943	4952	4611	4622

Figure 55 Data sheet for adhesive tapes